Flow of human blood through fabricated replicas of microvascular bifurcations
by Bruce Miles Fenton

A thesis submitted in partial fulfillment of the requirements for the degree of MASTER OF SCIENCE in CHEMICAL ENGINEERING
Montana State University


Abstract:
In view of the extremely limited knowledge of the relationships between the macroscopic rheological properties of blood and the microscopic behavior of the constituents of blood during flow through the actual geometries present in the microcirculation (such as bifurcations, capillary networks, etc.) vascular replicas of sections of rabbit ear blood vessels were studied.

The main objective of this study was to determine the feasibility of using these replicas in the mathematical prediction and subsequent measurement of the pressure flow relationships of human blood crossing a bifurcation.

Using both Newtonian (distilled water, S-3 silicone oil, and S-60 silicone oil) and non-Newtonian (red blood cell suspensions in plasma) fluids, differential pressures could be measured across the system and the effect of the flow distribution could be studied. The applicability of various mathematical models to non-uniform tapered tubes was investigated and it was determined that a "series of cylinders" approach was a close approximation for calculating pressure gradients across the tube (in reference to the specific vessel geometries studied.) Based on experimental results presented, it was concluded that the prediction of a large pressure drop at a bifurcation is not supported by the experimental data, but is instead directly contradicted, with the measured pressure gradient being almost exactly equivalent to that predicted in the absence of branching.

STATEMENT OF PERMISSION TO COPY

In presenting this thesis in partial fulfillment of the requirements for an advanced degree at Montana State University, I agree that the library shall make it freely available for inspection. I further agree that permission for extensive copying of this thesis for scholarly purposes may be granted by my major professor, or, in his absence, by the Director of Libraries. It is understood that any copying or publication of this thesis for financial gain shall not be allowed without my written permission.

Signature Bruce M Fenton

Date 9-9-75

# FLOW OF HUMAN BLOOD THROUGH FABRICATED REPLICAS OF MICROVASCULAR BIFURCATIONS

by

BRUCE MILES FENTON

A thesis submitted in partial fulfillment
of the requirements for the degree

of

MASTER OF SCIENCE

in

CHEMICAL ENGINEERING

Approved:

Head, Major Department

Chairman, Examining Committee

Graduate Dean

MONTANA STATE UNIVERSITY
Bozeman, Montana

December, 1975

# ACKNOWLEDGMENTS

The author would like to thank the entire faculty of the Chemical Engineering Department of Montana State University for their constant advice and encouragement. Special thanks are due Dr. G. R. Cokelet for his never-ending supply of answers (and equally endless supply of questions). In addition I would like to thank Dick Moran, at the Physician's Lab, for his phlebotomies at a moments notice, and Sue for typing her little heart out on my thesis.

Financial support for this study was provided by the National Heart and Lung Institute, Grant # HL 12723.

TABLE OF CONTENTS

TABLE OF CONTENTS (continued)

# LIST OF TABLES

# LIST OF FIGURES

## ABSTRACT

In view of the extremely limited knowledge of the relationships between the macroscopic rheological properties of blood and the microscopic behavior of the constituents of blood during flow through the actual geometries present in the microcirculation (such as bifurcations, capillary networks, etc.) vascular replicas of sections of rabbit ear blood vessels were studied.

The main objective of this study was to determine the feasibility of using these replicas in the mathematical prediction and subsequent measurement of the pressure flow relationships of human blood crossing a bifurcation.

Using both Newtonian (distilled water, S-3 silicone oil, and S-60 silicone oil) and non-Newtonian (red blood cell suspensions in plasma) fluids, differential pressures could be measured across the system and the effect of the flow distribution could be studied. The applicability of various mathematical models to non-uniform tapered tubes was investigated and it was determined that a "series of cylinders" approach was a close approximation for calculating pressure gradients across the tube (in reference to the specific vessel geometries studied.)

Based on experimental results presented, it was concluded that the prediction of a large pressure drop at a bifurcation is not supported by the experimental data, but is instead directly contradicted, with the measured pressure gradient being almost exactly equivalent to that predicted in the absence of branching.

# INTRODUCTION

In an attempt to quantitatively understand both the microscopic and macroscopic behavior of blood as it flows through the human body, much effort has been devoted to investigations of the distribution of the circulatory system. The question of blood flow distribution is thought to be an important one for several reasons. Most importantly perhaps is the fact that in organs where transfer of vital materials takes place, such as the lungs, alterations in blood flow distribution may affect the well-being of the entire organism.

## Components of the Blood

Human blood is a suspension of formed elements, in a liquid medium known as plasma. The formed elements consist of red blood cells (RBC's), white blood cells, and platelets. The red blood cells, also known as erythrocytes, make up the major portion (about 97%) of the cell volume and have the undeformed shape of a biconcave disc. The cells average approximately eight microns in diameter and two microns in thickness at the widest point. Since the red blood cell is essentially a thin membrane filled with fluid, it is very flexible and easily deformed during flow.

The plasma is the liquid portion of the blood and represents approximately 55 per cent of the volume of whole blood in healthy

individuals. It is composed of 90 per cent water, with various chemical substances in solution. These include proteins, lipids, carbohydrates, non-protein-nitrogen compounds, and inorganic materials.

The white blood cells, or leukocytes are the least numerous but the largest of the cells, and the platelets are the smallest. Since the leukocytes have been shown to exert a negligible effect on flow properties when in normal physiological concentrations, these cells and the platelets are removed for the purpose of this study. This resulting absence of platelets also reduces the tendency for the blood to form aggregates.

The hematocrit (ht) is defined as the volume per cent red blood cells per volume whole blood. It can be determined by centrifuging a capillary tube full of blood and measuring the relative length of the packed red cells to total volume. This method is 99 per cent accurate, as approximately one per cent of the RBC volume is trapped plasma. After removal of the platelets and leukocytes, various hematocrits are obtained by mixing different suspensions of RBC's in plasma.

Plasma Skimming

It has been reported by many investigators that the percentage of red blood cells in the whole blood (hematocrit) is lower in the capillary bed than in the larger blood vessels of the central circulation,

although the extent to which the hematocrit is reduced varies from organ to organ (Lawson, 1967). This reduction in concentration, which occurs in the more slowly flowing branch of a bifurcation, has come to be known as plasma skimming and has been the object of a variety of *in vivo* and *in vitro* studies. Gelin (1963) perfused blood through branched capillary models to permit closer analysis of plasma skimming and the flow properties of the blood, while eliminating physiological influences. Bugliarello and Hsiao (1964) flowed a suspension of spheres through a bifurcation as a simplified macroscopic model of the flow of blood and found that the concentration in the side branch was generally lower than in the main branch. Johnson (1971) used *in vivo* studies to measure average blood opacities in capillaries of the cat mesentery. Using these opacities as a quantitative measure of the hematocrit, vessels within the capillary network showed sizable differences in opacity. It was found that the capillaries with the higher red cell velocity also had the higher opacities. The reader is cautioned at this point that these opacity readings are not necessarily a measure of plasma skimming exclusively. As was well documented by Barbee and Cokelet (1971) the presence of a reduced hematocrit inside vessels less than 300 microns is a normal phenomena (known as the Fahraeus effect) even in the absence of bifurcations.

For both the *in vivo* and *in vitro* studies, there are advantages and disadvantages. *In vivo* studies have the advantage of exact

simulation of the actual vessel characteristics and geometries, but the accompanying disadvantages of reduced control of specific parameters and possible experimental interference with the normal hormonal, local, and neurological controls of the vascular system. *In vitro* studies, on the other hand, have permitted greater control of a number of the parameters affecting plasma skimming but have neglected the effects of such variables as vessel wall permeability and elasticity, pulsatile flow, and inertial effects due to actual vessel geometries (including curvature and taper).

In an effort to obtain the best features of both *in vitro* and *in vivo* measurements, the present study utilizes hollow vascular replicas formed from polyester resin (see Cokelet and Meiselman (1975)).

> The advantages of this type of flow system over the comparable *in vivo* preparation are its stability, transparency, the constancy of the geometry of the network of vessels under varying flow conditions, the impermeability of the walls of the flow channels, and the realistic, real-size representation of the vascular system. Not only can experimental blood flow data obtained from such a replica be compared with theoretical models of vascular systems, but contributions to flow resistance from such *in vivo* factors as vessel distensibility and vessel wall permeability can be assessed by the comparison of data obtained with *in vivo* and replica systems.

In view of the extremely limited knowledge of the relationships between the macroscopic rheological properties of blood and the microscopic behavior of the constituents of blood during flow through the actual geometries present in the microcirculation (such as bifurcations, capillary networks, etc.) vascular replicas should prove especially useful in defining the parameters involved. This type of research could become particularly helpful in understanding pathological situations.

Research Objectives

The main objective of this study was to determine the feasibilty of using vascular replicas in the study of the pressure/flow relationships of human blood crossing a bifurcation.

Originally, the principle emphasis for this research was to have been on plasma skimming and the resultant erythrocyte distribution across a bifurcation. Attempts were to have been made to determine whether correlations could be found between some of the variables which could not be investigated using large scale models; in particular, the shape and flexibility of the red blood cells. As the work progressed however, it was seen that both of the models selected were in a size range too large for the occurrence of any signifigant plasma skimming. From this point on, the focus was on mathematically defining the

differential pressure across a bifurcation using both Newtonian and non-Newtonian fluids. From this work, it was hoped that the various parameters affecting this pressure gradient could be determined; in particular, the effect of the fractional flow through the side branch of the bifurcation.

# EXPERIMENTAL APPARATUS AND PROCEDURE

The major portion of the research for this project was performed using two models for the study of pressure/flow relationships of various fluids (including human blood), and one for the measurement of the reduction in hematocrit present inside a small vessel, a phenomena known as the Fahraeus effect (see Barbee and Cokelet, 1971). Each of these phases of the research will be discussed separately, including details for the fabrication of the vascular replicas used.

## Blood

Human blood was obtained in ACD anti-coagulant by normal blood bank procedures without preference to specific types. Suspensions of red blood cells (RBC's) in plasma were prepared by 1) centrifugation of whole blood (using a Sorvall RC2-B automatic refrigerated centrifuge) at 5000 rpm for 15 minutes, 2) removal of platelets and leukocytes using a large diameter hypodermic needle and syringe, and 3) similar separation of red blood cells from plasma. Various hematocrits were then obtained by mixing specific volumes of RBC's and plasma together.

## Viscosity Measurements

The viscometer used was a Wells-Brookfield Micro Viscometer (cone and plate type), which was calibrated using the S-3 viscosity standard. Measurements were made on each blood sample at shear rates of 300, 750, and 1500 inverse seconds, at the recorded run temperature.

Viscosity measurements were also made using the GDM viscometer. This viscometer is a concentric cylinder type that is used to make viscosity measurements of RBC suspensions at shear rates from .06 to 60 inverse seconds. It was designed by Gilinson, Dauwalter, and Merrill, precisely for the measurement of non-Newtonian properties, and has a precision of nearly .1% for stress measurements. Torque/rotational speed data were reduced to shear stress-shear rate values by use of a computer program utilizing the Krieger-Elrod equation (see reference 9).

Calibration Techniques

Nominal flow rates were available for the Harvard Apparatus syringe pump, but for each specific syringe, more accurate rates were found by measuring mercury displacements at a number of different flow rates.

The pressure transducer was calibrated using a mercury manometer. For this model, actual induced pressures were recorded along with the accompanying digital voltmeter readings. A statistical least-squares

computer program was then used to correlate the experimental data and obtain straight line equations for each of the necessary attenuations of the amplifier. This calibration was checked periodically and readjusted as necessary.

Fabrication of Vascular Replicas

The method for fabricating the vascular replicas used in this study is thoroughly described elsewhere by Cokelet and Meiselman (1975), whose work can be briefly summarized as follows:

Ears obtained from male New Zealand rabbits are perfused, in sequence, with three liquids: (1) isotonic saline, to wash the blood out of the vascular system; (2) silicone oil, to provide a more favorable interface for the gallium; and (3) gallium, to form a replica of the vascular system.

Since gallium has a melting point of 29.8 C, it could be injected into the blood vessels in a liquid state and then allowed to solidify at normal room temperature. After solidification of the gallium, an enzymatic process was used for removal of the ear tissue. This process required from three to six weeks and utilized a protein denaturing solution of urea and $CaCl_2$ and a solution of pancreatin in a phosphate buffered saline. The tissue was subjected to a sequence of alternate solutions, repeated until all of the tissue

was removed from the gallium. The gallium network could then be separated into the desired bifurcations, which were then cast using a polyester resin (Silmar Polyester Resin S-40, Vistron Corp., with MEC catalyst, Norac Co.).

When the resin had hardened, holes were drilled into the vessels and the gallium was removed using first hot water and then a concentrated solution of hydrocholoric acid. This left only the hollowed out replication of the circulatory system, which was a transparent, impermeable, three-dimensional replica of the desired vessels. Reproducibility of the vascular sections was so keen, that actual endothelial cells could be seen in scanning electron micrographs of the model along with banding suggestive of vascular smooth muscle.

Model I Apparatus

For this portion of my research, an experimental setup was used as shown in Figure 1. This apparatus consisted of a syringe pump, connecting sections of polyethylene tubing, a polyester resin block containing a hollow replica of a section of rabbit-ear blood vessel, and a pressure transducer with accompanying amplifier and digital voltmeter readout.

Brief descriptions of the various components are as follows:

(1) The syringe pump was a Harvard Apparatus Co. Model 902

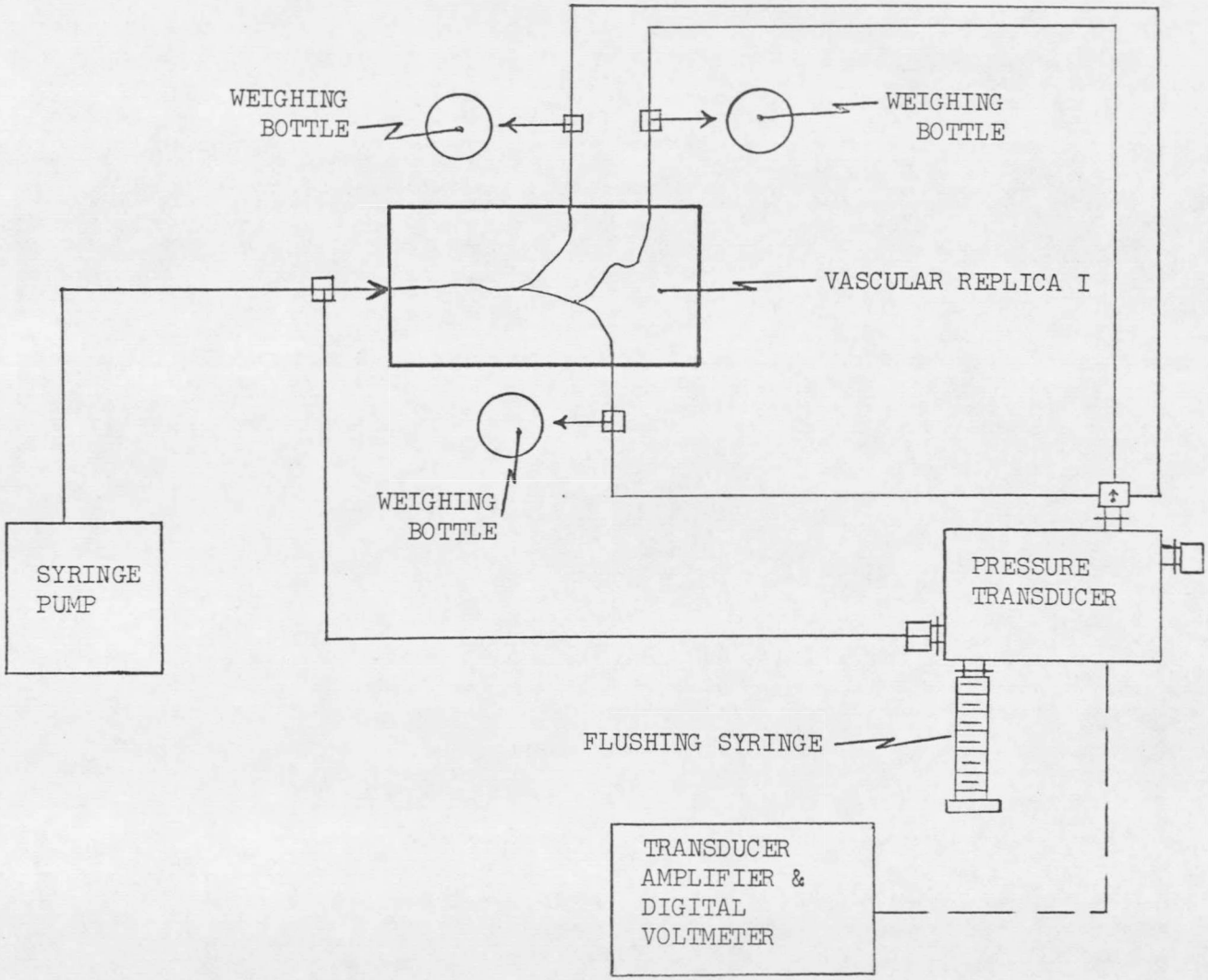


Figure 1. Schematic of Model I Apparatus

Infusion/withdrawal pump, which when fitted with 30 and 50 ml gas-tight syringes, could provide volumetric flow rates ranging from .0154 to 117.3 ml/minute.

(2) Connecting tubing for fluid flow was .105 inch medical grade polyethylene tubing (Becton, Dickinson, and Co.) with two-way and three-way valves and connecting fittings (Hamilton Co.).

(3) Connecting tubing for the pressure transducer leads was .023 inch I.D. polyethylene tubing. This particular size was chosen in order to eliminate air bubbles throughout the system and was filled with the fluid being tested (except in the case of red blood cell suspensions, in which case the leads were filled with plasma).

(4) The transducer used was a Sanborn Model 267BC differential pressure transducer (permitting both absolute and differential measurements) attached to a Sanborn Model 311A transducer amplifier. A Systron-Donner digital voltmeter was also added for instantaneous readout of the amplified transducer voltage.

(5) A 30 ml flushing syringe was utilized for the elimination of any air bubbles in the transducer and accompanying leads before commencement of a run.

(6) Mass flow rates through each of the branches were determined using three weighing bottles and a stop watch.

(7) Connections from the outside of the polyester resin model to the actual vessel inside were made using three 27 gauge blunt

hypodermic needles cemented in place using epoxy hardener.

Model II Apparatus

The apparatus for this model was similar to that used for Model I, although there was one major improvement to the system. In the preliminary experiments, all differential pressure measurements contained a certain amount of experimental uncertainty introduced by the drive fluctuations of the syringe pump. These fluctuations were caused by the slightly pulsatile flow of the pump, which in turn was produced by slight bows in the rotating screw mechanism which moved the syringe plunger. In order to minimize this uncertainty, a vessel was fabricated from glass tubing as illustrated in Figure 2. Fluids flowing from the syringe pump passed through this pressure damper, and then on to the vascular model. The sinusoidal pressure variations created by the pump were damped out by means of the air space above the blood reservoir, and after steady state had been reached, the transducer readout was seen to be essentially constant.

For measurements involving blood, it was also necessary to add a magnetic stirrer to the damper to prevent the settling out of RBC's when using low flow rates (as the experiment progressed, it was seen that a vessel of this type was required on the basis of its stirring capabilities alone, in order to provide a constant hematocrit feed

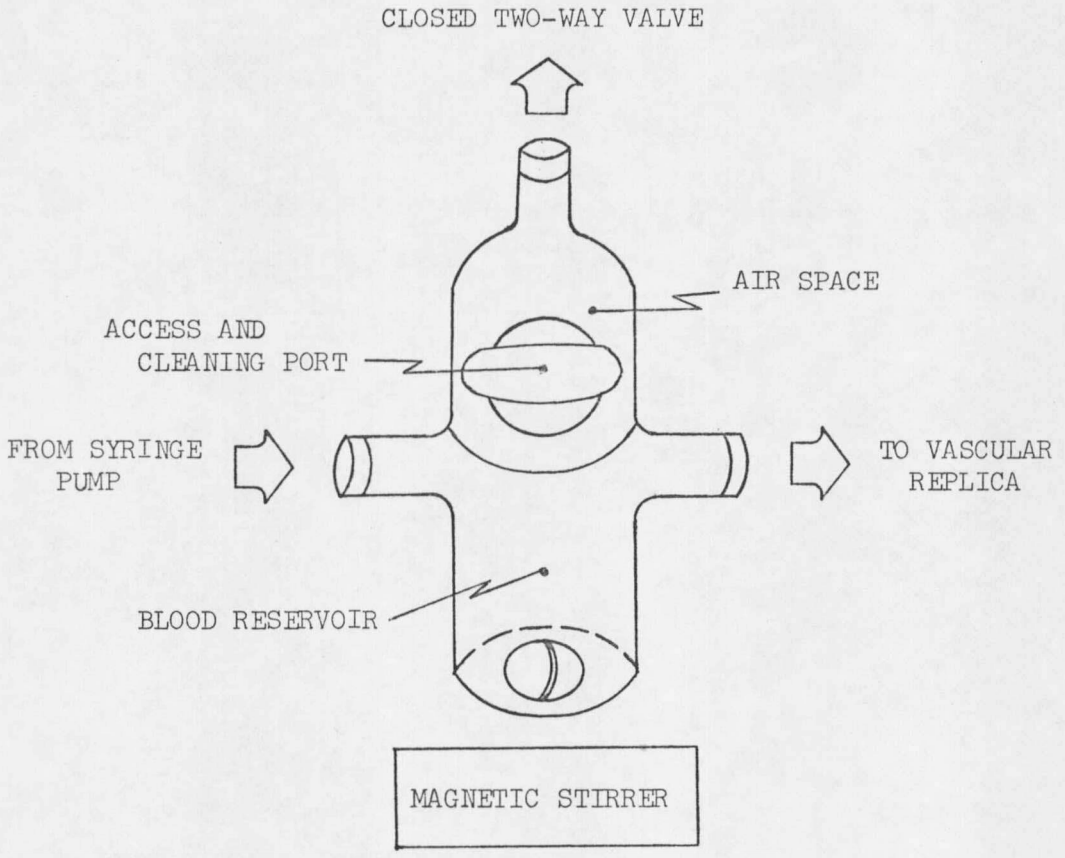


Figure 2. Pressure Damper and Stirrer

to the capillary model).

Also for Model II, a Hamilton two-way valve was added to the exit flow from the vessel replica in order to control the relative flow rates through the two branches by increasing the resistance through the main branch (see Figure 3). Flow rates were determined by means of weight and density measurements on the samples coming out of each of the branches, and pressure measurements were recorded on a Bausch and Lomb VOM-5 strip recorder and averaged over the duration of the run to define the absolute pressure at the tap.

After preliminary runs were performed using the two-way valve, it was seen that this method for controlling the relative flow through the branches was hardly ideal, for several reasons. Since comparatively high pressures were necessary to force significant percentages of the main branch flow into the side branch, the two-way valve had to be almost completely closed in all cases. This resulted in a build up of RBC's in the valve itself, and concomitant increase in the flow through the side branch. For this reason, steady-state values were impossible to obtain, flow distributions could not be accurately controlled, and runs could not be replicated.

The solution to this dilemma was to remove the two-way valve from the main branch exit and to insert, instead, a rising section of .105-inch polyethylene tubing. The outlet to this tubing was attached to an upright rod with a movable clamp so that the pressure head

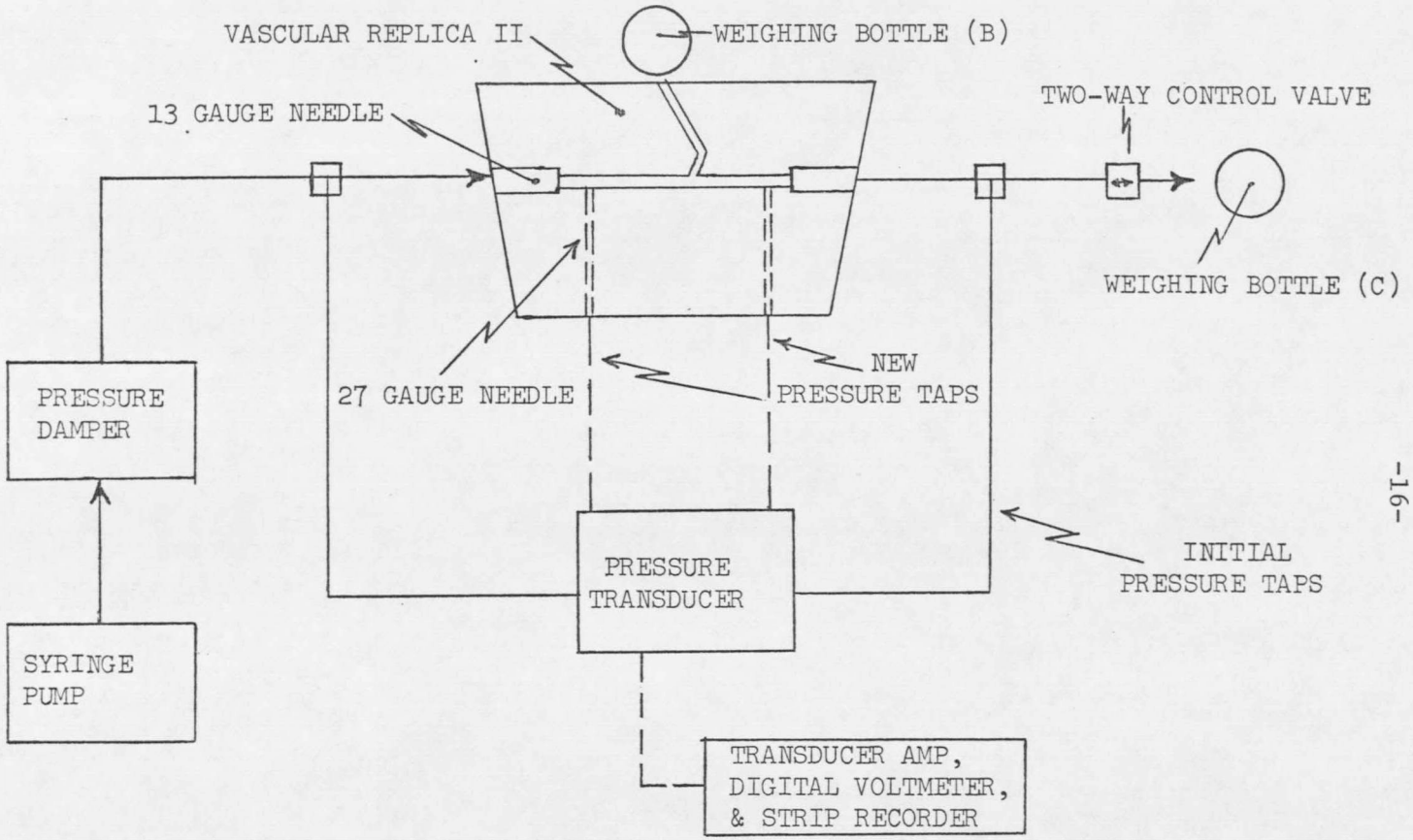


Figure 3. Schematic of Model II Apparatus

between the vascular replica and the tubing outlet could be varied. In this way, the pressure on the main branch outlet could be set to any specified value while steady-state flow was in progress. Runs were easily replicated and transducer readouts were constant to within .001 mV over the duration of a run. Zero values for the transducer were obtained by closing the valves leading to and from the vessel model.

For Model II, an extra degree of accuracy was obtained in calibrating the pressure transducer by using a Dwyer Instruments Hook Gage instead of the crude Hg manometer used for Model I. This hook gage permitted pressure measurements accurate to approximately .01 mm Hg, which was even more accurate than the digital voltmeter could be read (.5 mm Hg in most cases). Calibration curves were again obtained by means of a statistical least-squares program and a typical plot of the digital voltmeter reading (volts) versus the absolute pressure (mm Hg) is shown in Figure 4. For this data, the plot obtained by the program fits the following equation:

$$DVM = .005912\ P + .002202$$

where DVM is the digital voltmeter reading (in mV) and P is the corresponding pressure (mm Hg).

Model Dimensions

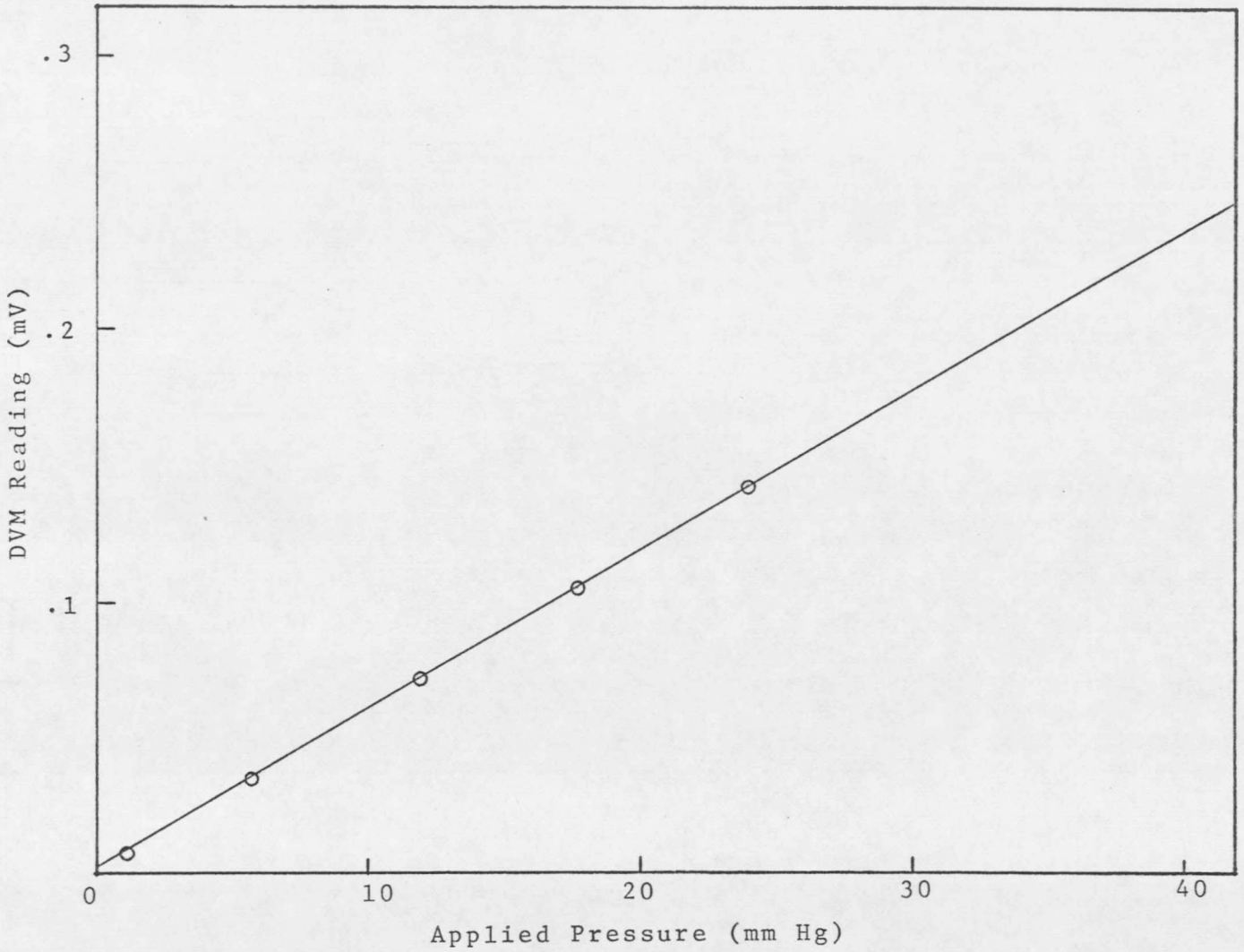


Figure 4. Pressure Transducer Calibration Curve

The linear dimensions of each model were determined by means of photographic enlargements (with accompanying metric scale) which were three to four times the original model size. The pertinent lengths were then measured using a computer-connected planimeter on the enlargement, and the diameters of the vessels were measured from the photomicrographs.

Model II is shown in Figure 5. It consisted of a main branch of approximately 905 microns and a tapering side branch which varied from 146.5 to 194.7 microns. Measurements of the tapered diameters were made (after the completion of all experimental study) by milling off specific lengths of the capillary replica and photographing the exposed vessel lumen under a metallurgical microscope with an accompanying micrometer scale. Seven slices were cut along the side branch and two along the main branch.

Experimental Measurements

For each run, measurements on the system included the volumetric flow rates through each of the branches, entrance and exit hematocrits (for the blood runs), and differential pressure measurements across the various bifurcations (for the distilled water runs). The hematocrits were found by means of the standard technique of centrifuging the samples in micro-hematocrit tubes (about 10,000g for ten min.) and measuring the volume of red blood cells per volume of cells and plasma. Pressure measurements were found both by utilizing the differential

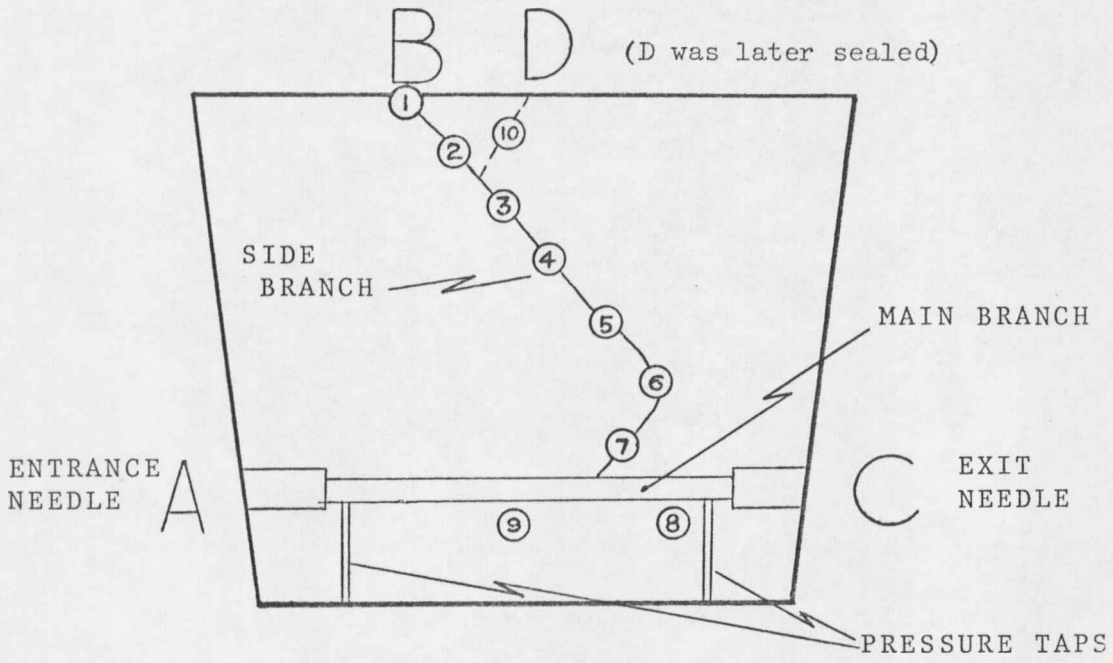


| # | Diameter | (measured from photomicrographs taken while slicing model at completion of runs) |
|---|---|---|
| 1 | 160.4 | |
| 2 | 151.5 | |
| 3 | 169.9 | Average = 174 microns |
| 4 | 180.2 | (assuming constant dia. from point 7 to main branch) |
| 5 | 188.5 | |
| 6 | 146.5 | |
| 7 | 194.7 | |
| 8 | 907.9 | Average = 905 microns |
| 9 | 902.3 | |
| 10 | 90.0 | =(from preliminary photos) |

Figure 5. Model II Dimensions

capabilities of the transducer and also by measuring the absolute pressures during the run and subtracting out the zero-flow reading.

Model II utilized two certified viscosity standards, Viscosity Standards S-3 and S-60 from the Cannon Instrument Company, for which viscosity and density data were well defined at all of the experimental temperatures studied. For the pressure/flow distribution runs made on the RBC suspensions, experimental measurements included: the temperature, branch and downstream hematocrits, density, mass flow rates, absolute pressure at the tap, and viscosity data.

For the initial pressure correlations, the side branch (B in Figure 3) was sealed off so all flow was through C. In an effort to better correlate the experimental pressure drops to the calculated values, transducer pressures were measured from a number of different taps. Initially, the taps were connected directly to two three-way valves (connected to 13 gauge hypodermic needles leading from both sides of the model vessel). Finally however, taps were drilled directly into the vessel walls (see Figure 5) and two 27 gauge blunt needles were cemented into place flush with the vessel walls.

For differential pressure measurements through the side branch of this model, valve C was closed, and the fluid was allowed to flow out of branch B and into a reservoir of liquid at approximately the

same level as the exit. In this way, surface tension effects of the fluid droplets leaving the vessel could be eliminated (the actual level of the reservoir liquid was unimportant for low flow rates since its net effect on the transducer was consequently cancelled out by using this pressure head as the transducer zero at the completion of each run). For the blood runs, the fluid in the reservoir was an isotonic saline which prevented the subsequent hemolysis of the blood as it left the vessel.

Investigation of Fahraeus Effect

A concomitant study was performed on Model II in which an attempt was made to measure the hematocrit inside the side branch of the system. For these measurements, it was first necessary to determine the volume of the vessel. This was done both by the standard method of mercury displacement, and by using the various lengths and diameters of the system (from the photomicrographs and enlargements) to calculate the volume by averaging the various diameters of the tapering tube. From the mercury displacement, it was determined that the volume of the branch was .000310 ml, and from the photographs (using a cylinder of average diameter equal to 195 microns), the volume was determined to be .000376 ml. It was decided that the mercury determination was the more accurate of the two and dilutions were carried out on the basis of a branch volume of .000310

milliliter. From the measurements of the taper of the branch (made by actually slicing up the model) the true volume can most closely be estimated at .000274 ml (see Figure 5).

The basic procedure for the hematocrit measurements was performed using a Coleman Junior II Spectrophotometer and can be summarized as follow:

(1) The entire system was flushed with plasma in order to coat the vessel and tube walls to prevent RBC attachment.

(2) Using the syringe pump as shown in Figure 6, the system was filled with blood and allowed to reach steady state as indicated by the pressure transducer.

(3) Flow was next terminated using valve 1 and the side branch exit (point 3) was sealed using laboratory parafilm (American Can Co.).

(4) The main branch was next flushed using Drabkin's Reagent from the syringe attached to valve 1. Flushing was performed through point 6 so that pressure would not build up behind valve 5, forcing the seal from branch 3. Drabkin's Reagent is a cyanide solution which causes hemolysis (breakdown) of the RBC's, and converts hemoglobin to a form which more strongly absorbs light in the spectrophotometric hemoglobin analysis. This solution was used to remove all traces of cells from the main branch.

(5) Valve 4 was next closed and the blood cell suspension remaining in the side branch was flushed into a spectrophotometer

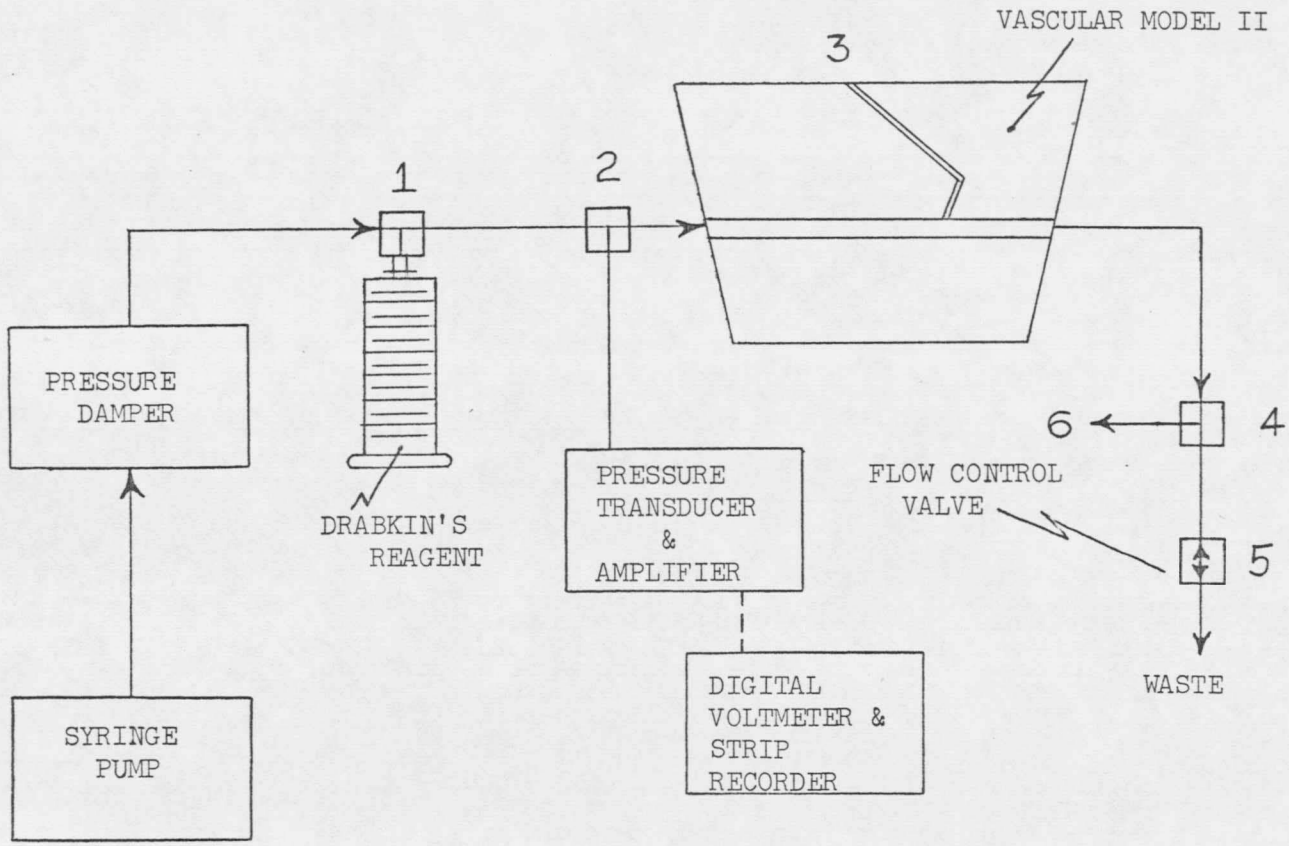


Figure 6. Schematic of Apparatus for Finding Tube Hematocrit

cuvette with approximately .2 ml of Drabkin's Reagent.

For each spectrophotometer measurement made, three runs were required in order to obtain enough of a blood sample to utilize the spectrophotometer. These three samples were combined with a total of .93 ml of Drabkin's Reagent to provide a dilution of 1000:1 (Drabkin's Reagent: blood). From this dilution, a spectrophotometer reading could be made of the per cent transmittance of the sample, and this value could be correlated graphically with the hematocrit of the blood sample (see Experimental Results and Discussion for further information on this procedure).

## EXPERIMENTAL RESULTS AND DISCUSSION

### Plasma Skimming Results

Preliminary work was done using Model I to see if plasma skimming could be observed at various distributions and entrance hematocrits. Since later experiments would rely on the tube hematocrits for pressure drop calculations, it was necessary at this point to determine that feed hematocrits were equivalent to discharge hematocrits for each of the different branches.

According to the conclusions of Gelin (1963): "Plasma skimming is only slight in capillary tubes wider than 200 microns and is marked only in capillary tubes narrower than 110 microns." Bugliarello and Hsiao (1964) used particles with an average diameter corresponding to a tube-to-particle ratio of approximately ten, which was selected as being in the range where the plasma skimming phenomenon has been observed to occur with blood (Gelin, 1963). This ratio corresponds to a vessel size of about eighty microns since the average RBC is about eight microns in diameter.

The minimum diameter of any of the vessels used in this study for differential pressure measurements was about 160 microns, but for some of the initial plasma skimming studies, a vessel of average diameter equal to ninety microns was also used. This larger vessel would not be expected to exhibit significant plasma skimming in any case, but

the smaller vessel could be expected to be a borderline case, according to the above criteria.

Using Model I, different branches were closed off for some of the runs, and exit hematocrits were measured using standard centrifugation techniques (see Table I and Figure 7). In general, lower hematocrits were observed in the more slowly flowing branches, but the differences between the various branches were never more than one hematocrit per cent, which is hardly significant.

For Model II, exit and branch hematocrits were measured for various entrance hematocrits and flow rates. Data from these runs is tabulated in Table II (see also Figure 5). Branch B is of average diameter 174 microns; D is ninety microns; and the main branch (A to C) is 905 microns. As with Model I, the branch with the smallest volumetric flow rate usually had reduced exit hematocrits in comparison to the other branches. Again, this difference is almost insignificant since none of the exit hematocrits varied by more than one or two hematocrit per cent. Thus, for both Models I and II, plasma skimming was seen to be a negligible parameter in relation to its effect on pressure measurements.

Also of interest in the study of the pressure flow relationships of blood is the reduced hematocrit noted inside very small vessels (Fahraeus effect). Although for vessels larger than about 300 microns the hematocrit inside the vessel is essentially the same as the feed

Table I. Preliminary Plasma Skimming Data (Model I)
V = 1.18 to 23.6 ml/min (total flow)

| Branch | Branch Diameter (microns) | % Flow | Exit Hematocrit % |
|---|---|---|---|
| A | 400 | 40.0 | 40.0 |
| B | 450 | 14.3 | 39.0 |
| C | 600 | 45.7 | 40.0 |
| A | 400 | 43.2 | 36.0 |
| B | 450 | 11.6 | 35.0 |
| C | 600 | 45.2 | 36.0 |
| A | 400 | 75.9 | 39.0 |
| B | 450 | 24.1 | 37.5 |
| A | 400 | 42.0 | 38.5 |
| B | 450 | 13.0 | 37.6 |
| C | 600 | 45.1 | 38.0 |
| A | 400 | 60.2 | 40.0 |
| C | 600 | 39.8 | 39.0 |
| A | 400 | 74.5 | 40.0 |
| B | 450 | 25.5 | 40.0 |

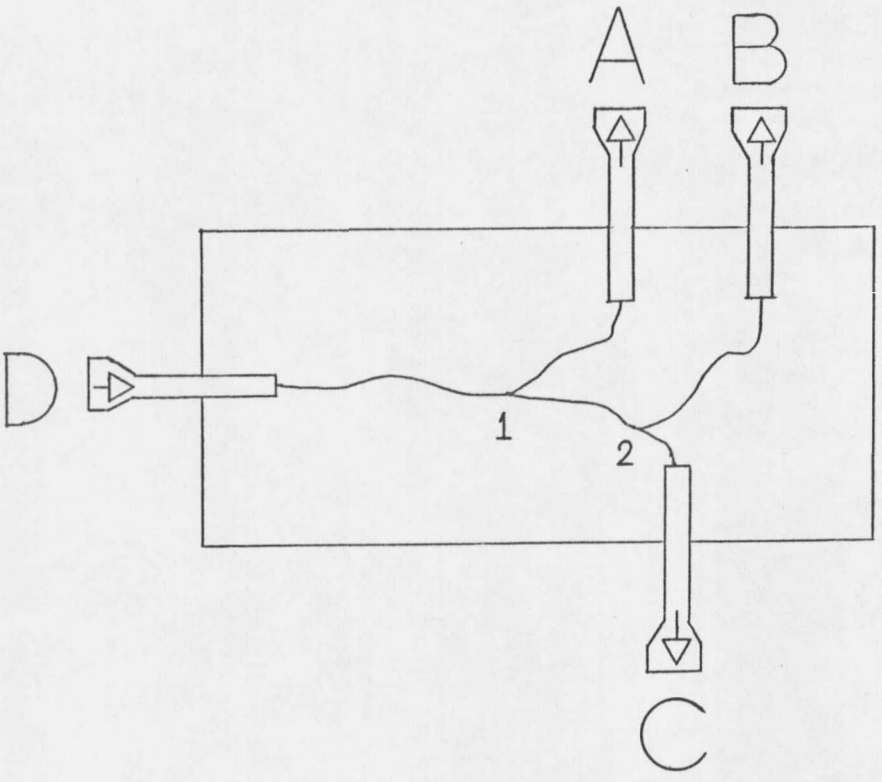


Figure 7. Vascular Model I

Table II. Preliminary Plasma Skimming Data (Model II)
V = 1.18 to 23.6 ml/min (total flow)

| Branch | Branch Diameter (microns) | Exit Hematocrit % |
|---|---|---|
| Feed A | 905 | 14.6 |
| Main C | 905 | No Flow |
| Side B | 174 | 13.7 |
| Side D | 90 | 14.5 |
| Feed A | 905 | 34.5 |
| Main C | 905 | 34.5 |
| Side B | 174 | 34.5 |
| Side D | 90 | 33.5 |
| Feed A | 905 | 16.0 |
| Main C | 905 | No Flow |
| Side B | 174 | 15.0 |
| Side D | 90 | 14.0 |
| Feed A | 905 | 17.0 |
| Main C | 905 | No Flow |
| Side B | 174 | 16.5 |
| Side D | 90 | 15.5 |

hematocrit, it has been well documented (Barbee and Cokelet, 1971) that in smaller vessels, a significant reduction from feed hematocrit to tube hematocrit is to be expected (see Figure 8). This effect can be explained by the lowered concentration of RBC's near the vessel wall caused by physical limitations. Because of the velocity distribution within the vessel, the resultant effect of the lowered RBC concentration near the wall is to cause more RBC's to be in the higher velocity tube center. Consequently, the RBC's have an average velocity that is higher than that for the plasma and the net result is a lower concentration within the vessel at any given time, in comparison to the feed and discharge concentrations.

In an effort to experimentally measure the reduced hematocrit present in the side branch of Model II (average diameter = 170 microns), spectrophotometer measurements were made on blood samples obtained from the side branch by the procedure described in the section on Experimental Apparatus and Procedure. To select the proper dilution range for the spectrophotometer, curves of 'per cent transmittance' versus 'wavelength of the light source' were first prepared using normal hematocrit human blood. From these curves, a wavelength of 427 microns and dilution of 1000:1 (Drabkin's Reagent : blood) were found to be optimal. Because of the very small volume of blood obtained from the side branch for each run, it was necessary to combine the volumes from three runs to have a dilution of 1000:1 and still have the necessary sample volume

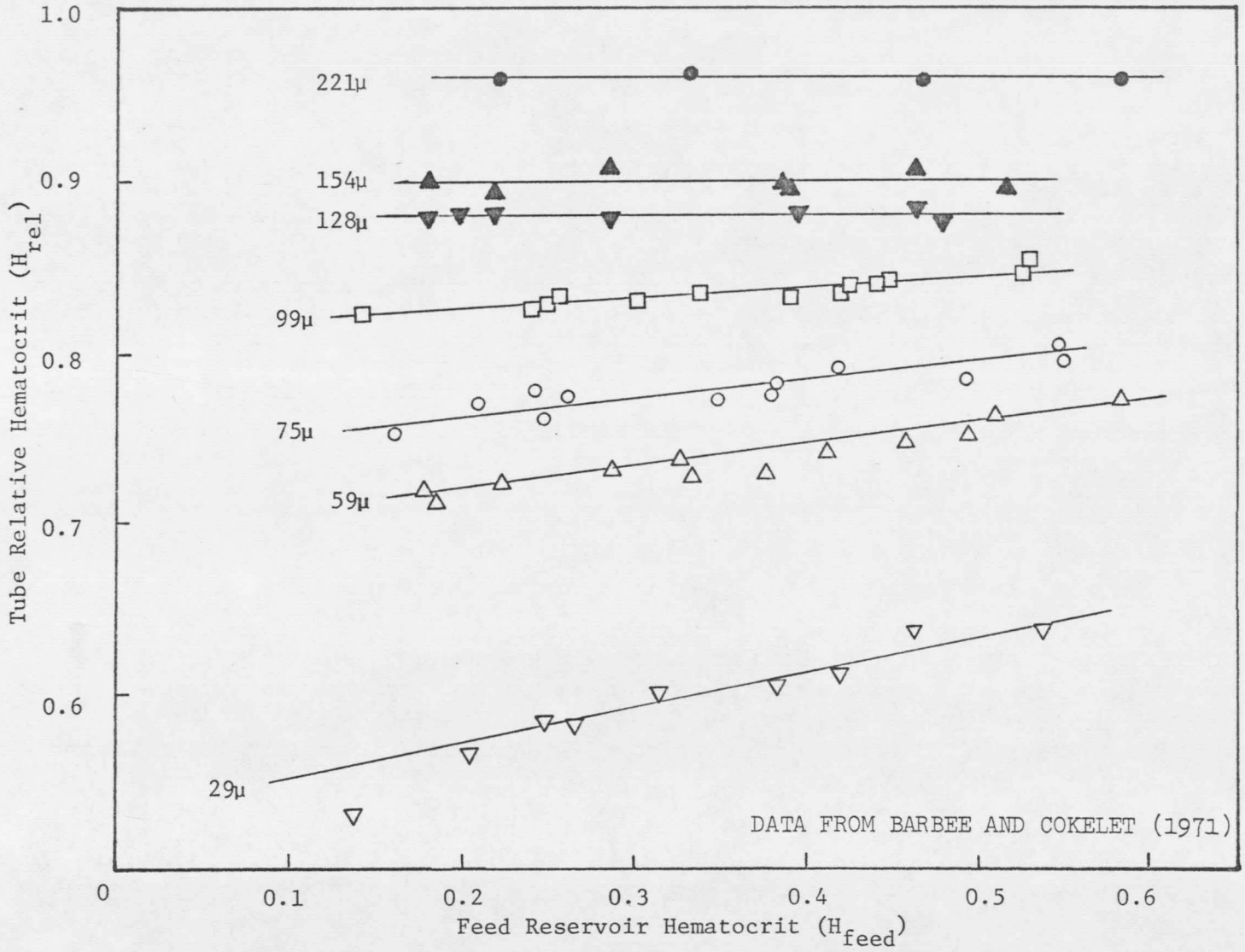


Figure 8. Tube Hematocrit versus Feed Hematocrit

for the spectrophotometer.

A calibration curve of log transmittance versus hematocrit was next plotted using blood samples (of known hematocrit) diluted 1000:1. The relationship between per cent transmittance and concentration is exactly expressed by the Lambert-Beer Law for the experimental procedure followed. This law states that the concentration (C) is proportional to the log of the reciprocal of the transmittance (T) by a factor K:

$$C = K \log (1/T)$$

This expression can be more simply expressed as:

$$C = -K \log T$$

so that from a plot of C versus log T, a straight line of slope -K results.

From a calibration curve of this type, measurements were made on the side branch at a variety of different hematocrits and flow rates. For this series of runs, flow was through both the side and the main branch and this flow ratio was varied, in an attempt to measure the effect of this parameter. Results for these runs are tabulated in Tables III, IV, and V, where $H_{feed}$, $H_{tube}$, and $H_{discharge}$ are the feed, tube, and discharge hematocrits respectively. $H_{tube}$'s were determined from spectrophotometric measurements and $H_{feed}$'s and $H_{discharge}$'s were determined by standard centrifugation techniques of the feed and discharge blood.

Using a statistical analysis of variance, it was determined that

Table III Spectrophotometric Analysis
Tube Hematocrit versus
Feed and Discharge Hematocrits
Flow Distribution: 70.3% Main Branch
29.7% Side Branch
Total Flow = 1.183 $cm^3$/min

| $H_{feed}$ | $H_{discharge}$ | $H_{tube}$ (side branch) |
|---|---|---|
| 40.2 | 40.1 | 40.0 |
| 27.4 | 27.2 | 24.0 |
| 27.0 | 27.2 | 25.0 |
| 20.8 | 20.8 | 19.5 |
| 36.7 | 36.8 | 38.0 |
| 38.8 | 38.1 | 39.5 |
| 40.4 | 40.6 | 39.5 |
| 43.2 | 43.4 | 45.0 |

Table IV. Spectrophotometric Analysis of Tube Hematocrit versus Feed and Discharge Hematocrits
Flow Distribution: 62.6% Main Branch
37.3% Side Branch
Total Flow =.589 $cm^3$/min

| $H_{feed}$ | $H_{discharge}$ | $H_{tube}$ (side branch) |
|---|---|---|
| 42.2 | 41.8 | 44.5 |
| 35.4 | 34.3 | 37.0 |
| 53.1 | 51.1 | 54.5 |
| 15.6 | 14.8 | 13.7 |

Table V. Spectrophotometric Analysis of Tube Hematocrit versus Feed and Discharge Hematocrits
Flow Distribution: 82.3% Main Branch
17.8% Side Branch
Total Flow =.589 $cm^3$/min

| $H_{feed}$ | $H_{discharge}$ | $H_{tube}$ (side branch) |
|---|---|---|
| 36.8 | 36.7 | 43.0 |
| 48.3 | 47.2 | 42.5 |
| 27.0 | 26.1 | 21.0 |
| 27.2 | 26.6 | 31.0 |
| 36.3 | 35.9 | 34.0 |
| 45.0 | 44.6 | 40.0 |
| 38.9 | 38.7 | 36.0 |
| 39.2 | 39.2 | 35.0 |
| 36.8 | 36.5 | 35.5 |

there was no significant difference between the hematocrits inside the side branch, and the entrance and the exit hematocrits. Although this analysis does not verify the presence of a reduced hematocrit inside the vessel as predicted by Barbee and Cokelet (1971), neither does it necessarily contradict it since the predicted hematocrit reduction is small and the experimental uncertainty of these tests is relatively large. The net effect of the data is to point out the limitations of this particular experimental method for measurements of the tube hematocrit in very small microvascular models.

Differential Pressure Measurements (Model I)

In an effort to compare measured pressure drops in the system to calculated values, distilled water was next pumped through Model I. Water was chosen because of its well-defined flow characteristics. For laminar flow in a circular pipe, Poiseuille's Equation applies:

$$-\Delta P = \frac{128\ V\ \eta\ L}{\pi\ D^4} \qquad (1)$$

where V = volumetric flow rate; $\eta$ = viscosity; L = tube length; and D = tube diameter. This equation assumes steady, uniform flow, and applies to a fluid of constant viscosity.

From transducer measurements, differential pressures were measured across each of the branches as shown in Figure 7. Average diameters were found across each of the branches and pressure differences

were calculated using Poiseuille's Equation. Calculated pressure drops from point D to points A, B, and C were 42.5, 44.4, and 38.5 mm Hg when branch flow rates were: 5.32, 4.69, and 1.82 $cm^3$/min. The experimentally measured pressure drop for this particular run was 68.5 mm Hg, a value approximately 1.6 times as high as the calculated values.

Water was next run through branch A only, at a rate of 11.83 $cm^3$/min, resulting in calculated and measured pressure drops of 55.7 mm Hg and 87.0 mm Hg respectively. Again, the measured pressure drop was found to be much larger than the calculated value; 1.56 times as high in this case.

In an effort to eliminate entrance and exit effects through the needles and the effects of curvature and taper, a differential pressure was next measured across points 1 and 2 (as shown in Figure 7). This segment of the model is a straight, fairly uniform segment, of diameter equal to approximately 490 microns. For this run, all flow was through branch A, and branches B and C were used as pressure taps to the transducer. At a flow rate of 11.83 $cm^3$/min, the experimental pressure was found to be 30 mm Hg, while the calculated was 9.95 mm Hg; again, the measured pressure was much higher than predicted, this time by a factor of three.

At this point, it was finally concluded that the discrepancy between the measured and calculated values was probably being caused by the obvious roughness of the vessel walls, which was in turn caused by

the particular material used in casting this vessel (an alloy of bismuth, tin , and lead). To investigate the effect of wall roughness on the experimental procedure, another model was obtained in which the vessels were made using gallium, instead of the previous alloy, which resulted in smoother walls than before.

Differential Pressure Measurements (Model II)

Model II is illustrated in Figure 5. For the pressure-drop measurements, the upper two branches (B and D) were both sealed off, so that the pressure measurements were across a straight, fairly uniform section of vessel.

In an effort to better correlate the experimentally determined pressure drops to the calculated values, transducer readings were taken from a number of different taps. Initially, the transducer leads were attached directly to the two three-way valves on each side of the vessel model. (See Figure 3) For these measurements, another flow system was constructed consisting of two needles attached directly to each other, without a vessel in between. From transducer readings taken on this system at flow rates corresponding to those through the model vessel, the pressure drop through the needles and valves could be determined independently and subtracted from the original readings to obtain an approximation of the pressure drop through the

vessel alone. Tabulation of these measurements for various flow rates are shown in Tables VI, VII, and VIII for water, S-60 silicone oil, and S-3 silicone oil respectively. Also included in the tables are the ratios of the measured pressures to the calculated pressures for comparison purposes, and the Reynolds numbers. The appropriate equations for calculating pressure drops and Reynolds numbers were:

$$-\Delta P_{calc} = \frac{128\ V\ \eta\ L}{\pi\ D^4} \qquad (2)$$

$$Re = \frac{D\ \rho\ V}{\eta} \qquad (3)$$

As can be seen in the tables, measured values were almost always higher than the corresponding calculated values; in most cases, this discrepancy increases with increasing flow rates.

In a final effort to eliminate the effects of the needles and valves on transducer measurements, taps were drilled directly into vessel walls, as illustrated in Figure 3. Data from these runs are summarized in Tables IX and X, for S-60 silicone oil and S-3 silicone oil, respectively. Water was also tried for these tests, but the pressure drops across the system were so small (0.1 to 1.0 mm Hg) that they could not be accurately measured using the available transducer and amplifier.

Data from the S-60 silicone oil (Table IX) are graphed in Figure 9, in which the volumetric flow rates are plotted versus the differential pressures across the vessel. Two curves are drawn: one for the measured

Table VI. Comparison of Calculated and Measured $\Delta P$'s, for Taps Outside of the Vessel Model ($H_2O$)

L=.82 cm D=.0905 cm $\rho$ =.998 g/cm$^3$

| Re | V (cm$^3$/min) | $\Delta P_{measured}$ (mm Hg) | $\Delta P_{calculated}$ (mm Hg) | $\frac{\Delta P_{measured}}{\Delta P_{calculated}}$ |
|---|---|---|---|---|
| 129.1 | 5.894 | .52 | .37 | 1.41 |
| 259.1 | 11.83 | 2.10 | .73 | 2.88 |
| 516.1 | 23.56 | 6.31 | 1.46 | 4.32 |
| 1034. | 47.22 | 20.51 | 2.94 | 6.98 |

Table VII. Comparison of Calculated and Measured $\Delta P$'s, for Taps Outside of the Vessel Model (S-60 Silicone Oil).

L=.82 cm D=.0905 cm $\rho$ =.8738 g/cm$^3$
$\eta$=1.33459 poise T=21.5 C

| Re | V (cm$^3$/min) | $\Delta P_{measured}$ (mm Hg) | $\Delta P_{calculated}$ (mm Hg) | $\frac{\Delta P_{measured}}{\Delta P_{calculated}}$ |
|---|---|---|---|---|
| .0827 | .589 | 6.48 | 4.88 | 1.33 |
| .166 | 1.183 | 12.27 | 9.84 | 1.25 |
| .331 | 2.355 | 25.08 | 19.56 | 1.28 |
| .827 | 5.894 | 59.57 | 48.96 | 1.22 |

Table VIII. Comparison of Calculated and Measured $\Delta P$'s, for Taps Outside of the Vessel Model (S-3 Silicone Oil)

$L$=.82 cm  $D$=.0905 cm  $\rho$=0.8396 g/cm$^3$
$\eta$=.038995 poise  T=20.9 C

| Re | V ($cm^3$/min) | $\Delta P_{measured}$ (mm Hg) | $\Delta P_{calculated}$ (mm Hg) | $\frac{\Delta P_{measured}}{\Delta P_{calculated}}$ |
|---|---|---|---|---|
| 5.40 | 1.183 | .26 | .288 | .90 |
| 10.9 | 2.355 | .70 | .571 | 1.23 |
| 27.2 | 5.894 | 2.02 | 1.43 | 1.41 |
| 54.6 | 11.83 | 4.29 | 2.88 | 1.49 |
| 109. | 23.56 | 9.73 | 5.71 | 1.70 |

Table IX. Comparison of Calculated and Measured ΔP's with Taps Drilled Directly into Vessel (S-60 Silicone Oil)
L=.65 cm D=.0905 cm

| V ($cm^3$/min) | $\Delta P_{measured}$ (mm Hg) | $\Delta P_{calculated}$ (mm Hg) | $\frac{\Delta P_{measured}}{\Delta P_{calculated}}$ | η (poise) | T (C) | Re |
|---|---|---|---|---|---|---|
| .589 | 5.09 | 4.07 | 1.25 | 1.398 | 20.8 | .0826 |
| .589 | 5.09 | 4.14 | 1.23 | 1.426 | 20.5 | .0826 |
| 1.183 | 9.99 | 8.16 | 1.22 | 1.398 | 20.8 | .1660 |
| 1.183 | 10.34 | 8.32 | 1.24 | 1.426 | 20.5 | .1660 |
| 2.355 | 20.69 | 16.25 | 1.27 | 1.445 | 20.3 | .3304 |
| 2.355 | 22.96 | 16.57 | 1.39 | 1.426 | 20.5 | .3304 |
| 5.894 | 56.44 | 42.04 | 1.34 | 1.445 | 20.3 | .8269 |

Table X. Comparison of Calculated and Measured $\Delta P$'s with Taps Drilled Directly into Vessel (S-3 Silicon Oil)

L=.65 cm D=.0905 cm

| V ($cm^3$/min) | $\Delta P_{measured}$ (mm Hg) | $\Delta P_{calculated}$ (mm Hg) | $\frac{\Delta P_{measured}}{\Delta P_{calculated}}$ | $\eta$ (poise) | T (C) | Re |
|---|---|---|---|---|---|---|
| 2.355 | .27 | .44 | .61 | .0388 | 21.1 | - |
| 5.894 | 1.05 | 1.13 | .93 | .0391 | 20.8 | - |
| 5.894 | .53 | 1.31 | .47 | .0389 | 21.0 | - |
| 5.894 | .70 | 1.12 | .63 | .0383 | 21.6 | - |
| 5.894 | .88 | 1.13 | .78 | .0388 | 21.1 | - |
| 5.894 | .88 | 1.09 | .81 | .0373 | 22.5 | 28.4 |
| 5.894 | .35 | 1.07 | .33 | .0371 | 22.7 | 29.0 |
| 5.894 | .35 | 1.07 | .33 | .0369 | 22.9 | 29.0 |
| 5.894 | .53 | 1.09 | .49 | .0373 | 22.5 | 28.4 |
| 11.83 | 1.76 | 2.29 | .77 | .0391 | 20.8 | - |
| 11.83 | 2.28 | 2.28 | 1.00 | .0389 | 21.0 | - |
| 11.83 | 1.76 | 2.23 | .79 | .0383 | 21.6 | - |

Table X. (Continued)
Comparison of Calculated and Measured ΔP's with Taps Drilled Directly into Vessel
(S-3 Silicone Oil)
L=.65 cm D=.0905 cm

| V ($cm^3$/min) | $\Delta P_{measured}$ (mm Hg) | $\Delta P_{calculated}$ (mm Hg) | $\frac{\Delta P_{measured}}{\Delta P_{calculated}}$ | η (poise) | T (C) | Re |
|---|---|---|---|---|---|---|
| 11.83 | 1.93 | 2.26 | .85 | .0388 | 21.1 | - |
| 11.83 | 1.05 | 2.22 | .47 | .0380 | 21.8 | - |
| 11.83 | 1.23 | 2.22 | .55 | .0380 | 21.8 | - |
| 11.83 | 1.23 | 2.18 | .56 | .0373 | 22.5 | 56.9 |
| 11.83 | 1.58 | 2.16 | .73 | .0371 | 22.7 | 57.0 |
| 11.83 | .53 | 2.16 | .25 | .0369 | 22.9 | 58.0 |
| 11.83 | .79 | 2.18 | .36 | .0373 | 22.5 | 56.9 |
| 23.56 | 4.56 | 4.55 | 1.00 | .0391 | 20.8 | - |
| 23.56 | 5.61 | 4.53 | 1.24 | .0389 | 21.0 | - |
| 23.56 | 5.61 | 4.45 | 1.26 | .0383 | 21.6 | - |
| 23.56 | 5.09 | 4.51 | 1.13 | .0388 | 21.1 | - |
| 23.56 | 4.03 | 4.42 | .91 | .0380 | 21.8 | - |

Table X. (Continued)
Comparison of Calculated and Measured ΔP's with Taps Drilled Directly into Vessel
(S-3 Silicone Oil)
L=.65 cm D=.0905 cm

| V ($cm^3$/min) | $\Delta P_{measured}$ (mm Hg) | $\Delta P_{calculated}$ (mm Hg) | $\frac{\Delta P_{measured}}{\Delta P_{calculated}}$ | η (poise) | T (C) | Re |
|---|---|---|---|---|---|---|
| 23.56 | 4.21 | 4.42 | .95 | .0380 | 21.8 | - |
| 23.56 | 3.16 | 4.34 | .73 | .0373 | 22.5 | 113. |
| 23.56 | 3.86 | 4.32 | .89 | .0371 | 22.7 | 114. |
| 23.56 | 2.98 | 4.30 | .69 | .0369 | 22.9 | 115. |
| 23.56 | 3.16 | 4.34 | .73 | .0373 | 22.5 | 113. |
| 47.22 | 10.52 | 9.12 | 1.15 | .0391 | 20.8 | - |
| 47.22 | 10.52 | 9.06 | 1.16 | .0389 | 21.0 | - |
| 47.22 | 10.52 | 8.92 | 1.18 | .0383 | 21.6 | - |

Table X. (Continued)
Comparison of Calculated and Measured ΔP's with Taps Drilled Directly into Vessel
(S-3 Silicone Oil)
L=.65 cm D=.0905 cm

| V ($cm^3$/min) | $\Delta P_{measured}$ (mm Hg) | $\Delta P_{calculated}$ (mm Hg) | $\frac{\Delta P_{measured}}{\Delta P_{calculated}}$ | η (poise) | T (C) | Re |
|---|---|---|---|---|---|---|
| 47.22 | 10.52 | 9.04 | 1.16 | .0388 | 21.1 | - |
| 47.22 | 9.82 | 8.88 | 1.11 | .0380 | 21.8 | - |
| 47.22 | 9.99 | 8.88 | 1.13 | .0380 | 21.8 | - |
| 47.22 | 9.12 | 8.71 | 1.05 | .0373 | 22.5 | 227. |
| 47.22 | 8.94 | 8.66 | 1.03 | .0371 | 22.7 | 228. |
| 47.22 | 8.59 | 8.61 | 1.00 | .0369 | 22.9 | 230. |
| 47.22 | 8.56 | 8.71 | 1.41 | .0373 | 22.5 | 227. |

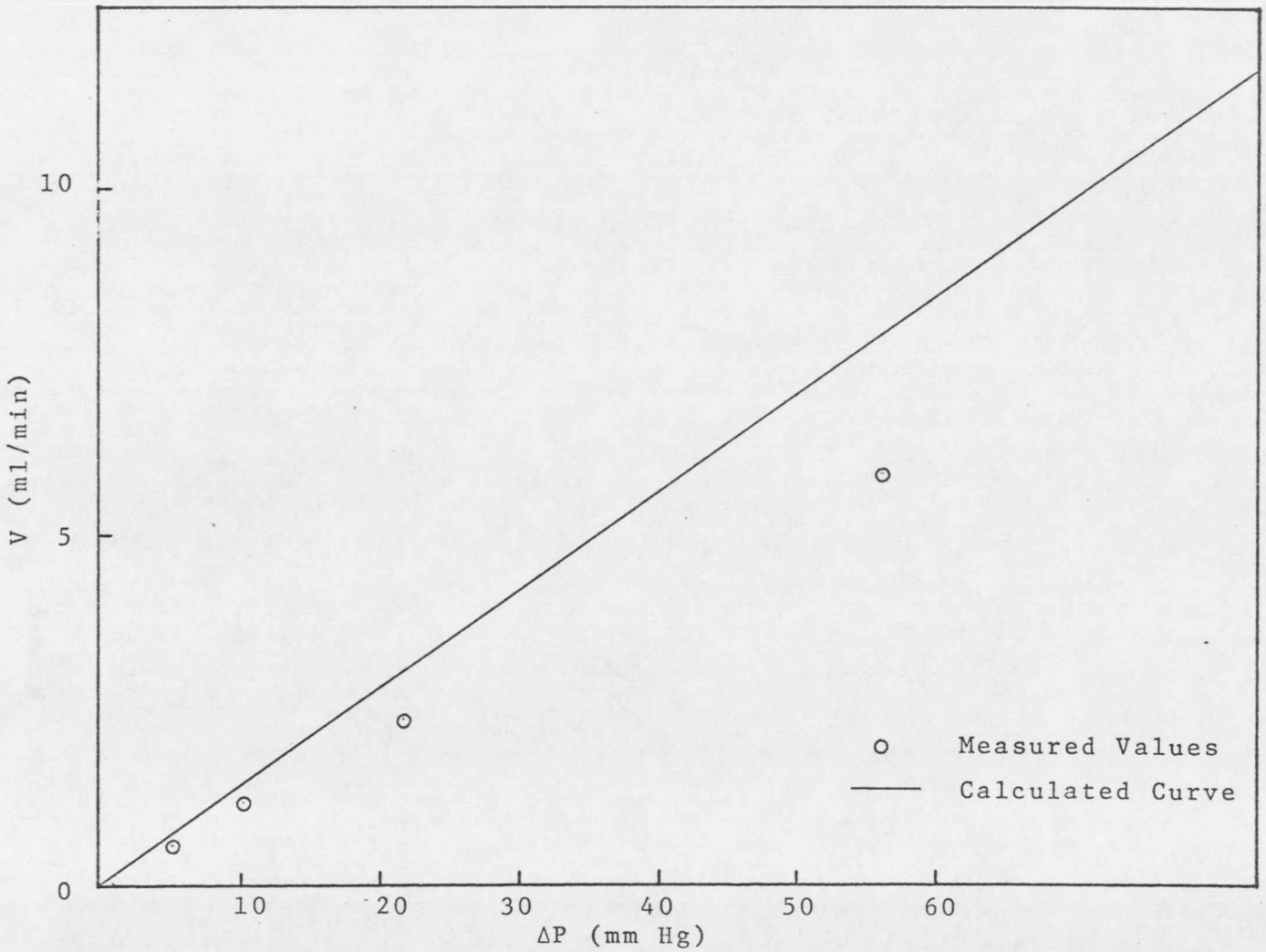


Figure 9. Comparison of $\Delta P_{measured}$ and $\Delta P_{calculated}$ over a Straight Vessel (S-60 Silicone Oil)

pressure values and one for the calculated values. Similar graphs were drawn for the S-3 silicone oil. In this case however, there was such scatter in the data, that at most flow rates ten runs were made and an average measured pressure was used in the plot. As can be seen in Figure 10, the average measured pressure values fit the calculated curve fairly well at each of the five flow rates tested.

A possible explanation for the deviations of the S-60 silicone oil data from the calculated line is that experimental techniques were not quite as refined at this point in comparison to later runs. Transducer readings were measured directly from the digital voltmeter instead of using a strip chart to find the average (as was later done), so that the accuracy of the resulting differential pressures was somewhat reduced. If a larger amount of data had been collected for the S-60 silicone oil and averaged (as was done with the S-3), it is likely that the resulting values would more closely fit the calculated line.

Tapered Tube Analysis

Because of the fact that the side branch is actually a non-uniform tapered tube, several methods were considered in attempting to calculate the pressure drop across the vessel. These methods will be discussed after a brief introduction to some of the approaches taken by other workers in this field.

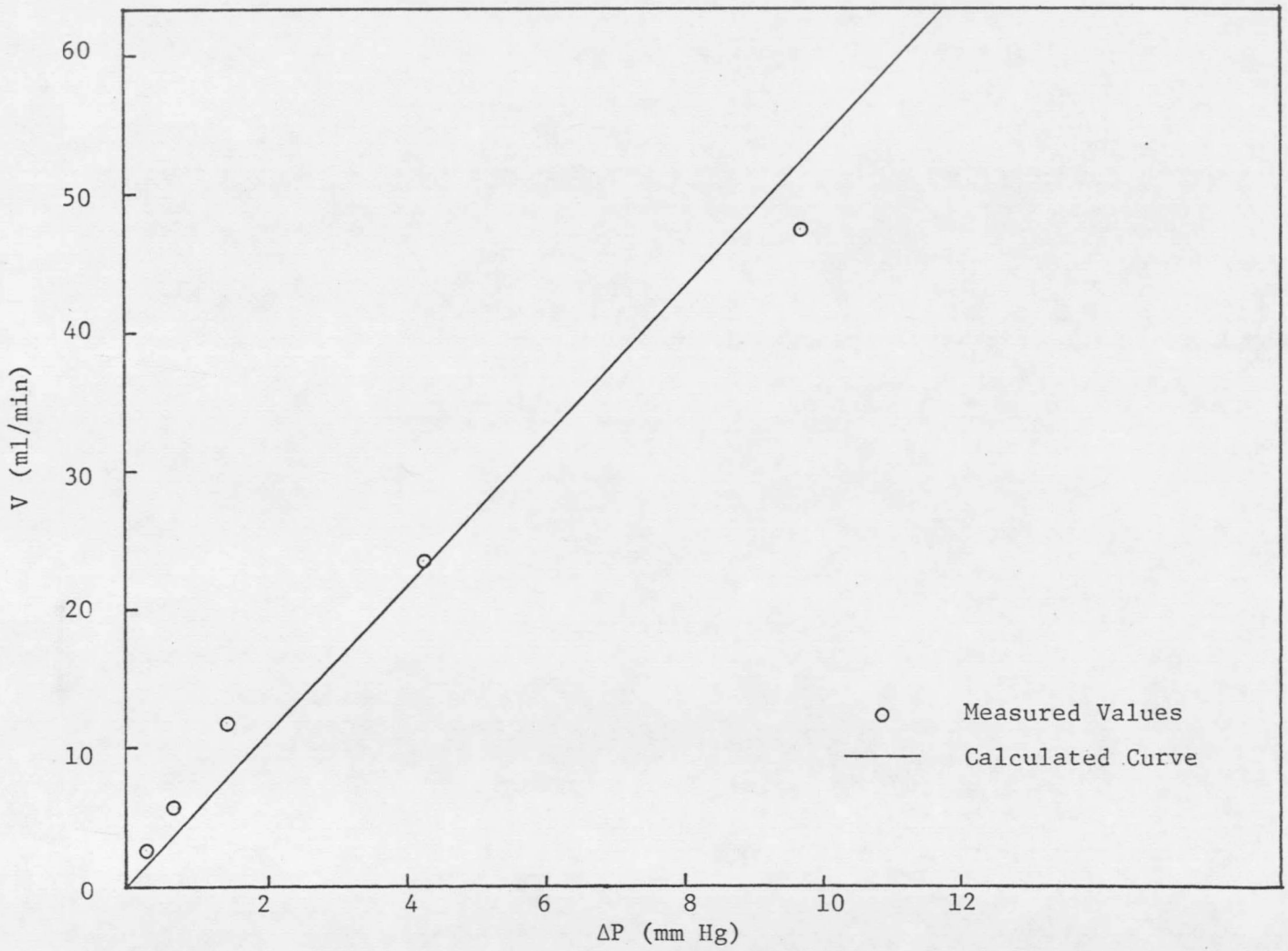


Figure 10. Comparison of $\Delta P_{measured}$ and $\Delta P_{calculated}$ through a Straight Vessel (S-3 Silicone Oil)

Although there have been numerous theoretical considerations of flow in tapered tubes, experimental work to confirm these predictions is still fairly scarce so that available models must be judged on their relative merits alone in attempting to choose a reliable method of solution. Cerny and Walawender (1966) considered the steady laminar flow of an incompressible non-Newtonian fluid in a uniformly-tapering tube of circular cross section. Their solutions included pressure flow relations for the cases of both pulsatile and steady flow in a rigid tube. Inertial terms were neglected in the Navier-Stokes equation, which would be a valid assumption in the case of the small vessel since the Reynolds numbers are small there. Walawender and Tien (1972) presented approximate pressure/flow relationships for the case of steady, laminar blood flow in small angle, uniformly tapering tubes. From their solutions for very slow and very fast flow, they derived a solution for a substantially extended flow range by adding an inertial correction term.

Charm and Kurland (1967) analyzed blood flow in non-uniform tapered capillary tubes by considering a model of increments of cylindrical tubes. If the yield stress of the blood and plasma marginal layer are both neglected, Poiseuille's equation results and the pressure losses in each segment can be calculated using mean diameters and summed. A similar approach was employed by Benis and Lacoste (1968) for the flow of a Casson fluid in a tapered vessel. They

made the assumption that the local pressure gradient at any point in the tube is the same as that in a uniform tube of the same diameter.

In general, for steady flow of a Newtonian fluid in a uniform rigid circular tube:

$$\tau_w = (8\ \eta\ \overline{U}) = \frac{\Delta P\ D}{4\ L} \qquad (4)$$

where $\tau_w$ is the shear stress at the wall; $\overline{U}$ is the reduced bulk average velocity in tube diameters/second; L is the length of the tube; and $\eta$ is the kinematic viscosity. If for flow in conically-tapered tubes it is assumed that (1) wall shear is a function of $\overline{U}$ only, and (2) the taper is uniform, equation (4) can be integrated to obtain the overall pressure drop (see appendix for full derivation):

$$\frac{\Delta P}{L} = \frac{128\ \eta\ V}{\pi\ D_{NM}^4} \qquad (5)$$

where

$$D_{NM}^4 = \frac{3(D_2-D_1)}{D_1^{-3} - D_2^{-3}} \qquad (6)$$

Equation (5) is precisely Poiseulle's equation, except for the substitution of the Newtonian mean diameter ($D_{NM}$) for the tube diameter.

To determine the reliability of using this equation for the prediction of measured pressure gradients in the vessel models of the present study, several test runs were made pumping a Newtonian fluid (plasma) through the side and main branches of Model II. For

these runs, the pressure gradients were measured across the side branch and compared to calculated values. In an effort to find the optimum mathematical model for the correlation of calculated and measured values, three methods were used for finding the calculated and measured values. In the first method, the average diameter of the tapered tube (as shown in Figure 5) was used to obtain a single mean diameter for a cylindrical tube (174 microns). For the second method, the tube was considered to be a series of seven cylinders in which each segment was approximated by an average diameter obtained from the end diameters of that segment. Individual pressure gradients were then determined across each cylindrical section using Poiseuille's equation, and the total pressure drop across the vessel was found by summation. The third and final method used the same "seven segments" approach but instead of using Poiseuille's equation for the individual pressure drops, equation (5) was used, with the Newtonian mean diameters substituted for the average cylindrical diameters of method two.

Data from each of these mathematical models, along with the flow rates and fractional flows through the side branch, are tabulated in Table XI and shown graphically in Figure 11. As can be seen in the figure, the best fit of the measured values is to the line obtained from method three, which was the one utilizing Newtonian mean diameters. Values from the series of cylinders (method two) are also a close correlation, however, and even those from the average diameter

Table XI. Comparison of $\Delta P_{measured}$ and $\Delta P_{calculated}$ (plasma flow) Across a Tapered Tube Using Various Mathematical Models

| V ($cm^3$/min) | $\Delta P_{measured}$ (mm Hg) | $\Delta P_{calculated}$ (method 1) | $\Delta P_{calculated}$ (method 2) | $\Delta P_{calculated}$ (method 3) |
|---|---|---|---|---|
| .0818 | 10.66 | 9.45 | 10.07 | 10.30 |
| .1238 | 15.89 | 14.31 | 15.24 | 15.59 |
| .1332 | 16.53 | 15.39 | 16.40 | 16.78 |
| .1724 | 21.64 | 19.92 | 21.22 | 21.72 |
| .2391 | 30.47 | 27.63 | 29.43 | 30.12 |

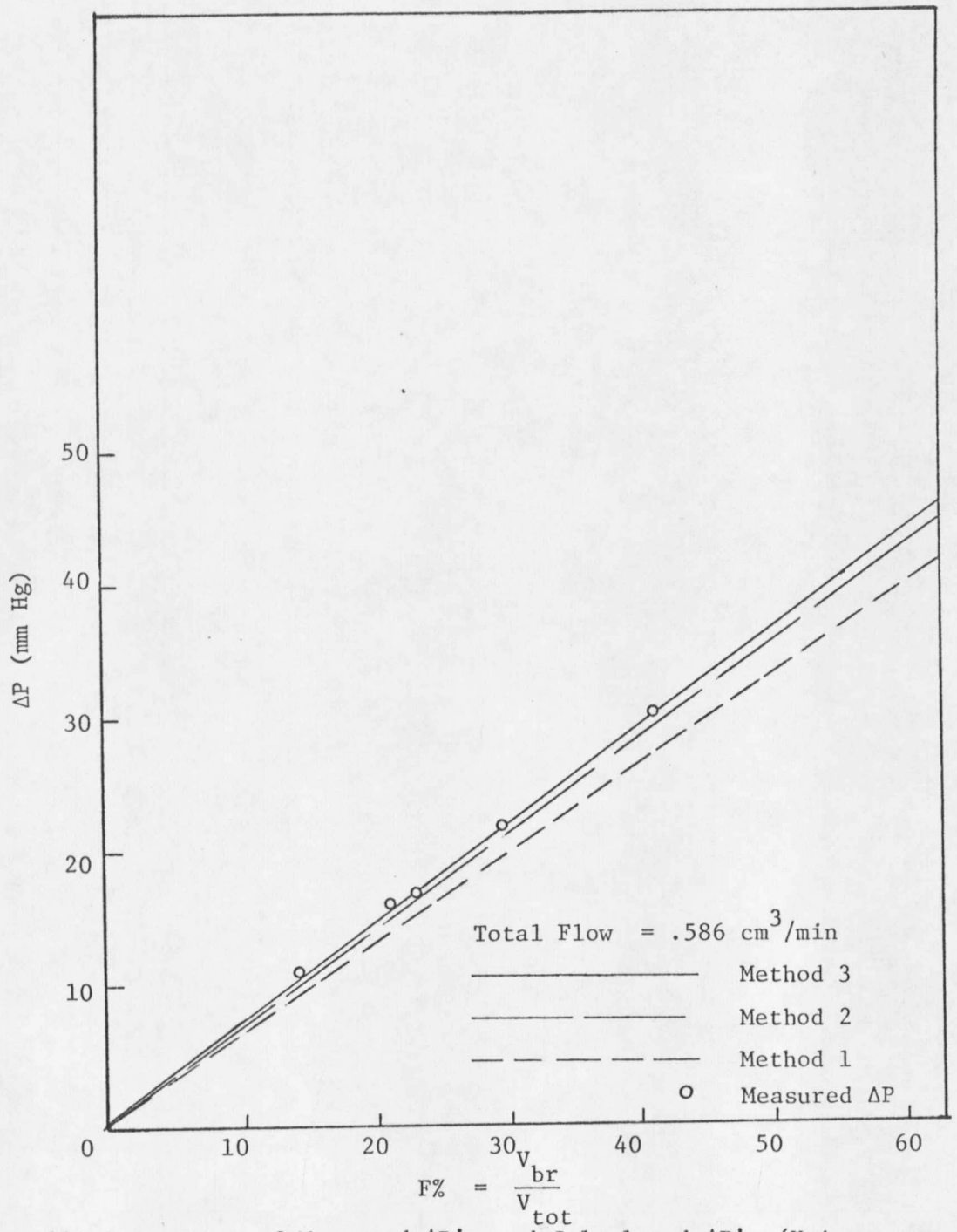


Figure 11. Comparison of Measured ΔP's and Calculated ΔP's (Using Various Mathematical Methods) for Plasma Flow Through the Side Branch of Model II.

cylinder (method one) are not far off.

Based on the above analysis, it was decided that the "series of cylinders" model was a very close approximation of the actual tapered tube. As a further check on the reliability of approximating a tapered tube by a cylinder of diameter equal to the tapered tube's mean diameter, reference is made to the work of Walawender and Prasassarakich (in press). They present analytical considerations that show that "the approximation of a tapered vessel by a cylindrical tube is increasingly in error as the radius ratio increases, but is lessened by the presence of non-Newtonian behavior of the fluid." For the purpose of his analysis, Walawender defines two variables, n and $B_m$, as follows:

$$n = \frac{R_1}{R_2}$$

where $R_1$ and $R_2$ are the radii at opposite ends of the tapered tube, and

$$B_m = \text{Bingham number} = \frac{\pi R_1^3 \tau_y}{Q S^2}$$

where $\tau_y$ is the yield stress, S is the Casson constant, (for the Casson fluid model), and Q is the flow rate. Figure 12 is taken from Walawender (in press) and is a plot of $\Delta$ (the ratio of $\Delta P_{tapered}$ to $\Delta P_{cylindrical}$) versus n. For the tapered tube being investigated in the present study, the maximum value of n is equal to 1.33, which corresponds to a $\Delta$ value of about 1.06 (see Figure 12), for the highest possible Bingham number. For this vessel, therefore, it can be

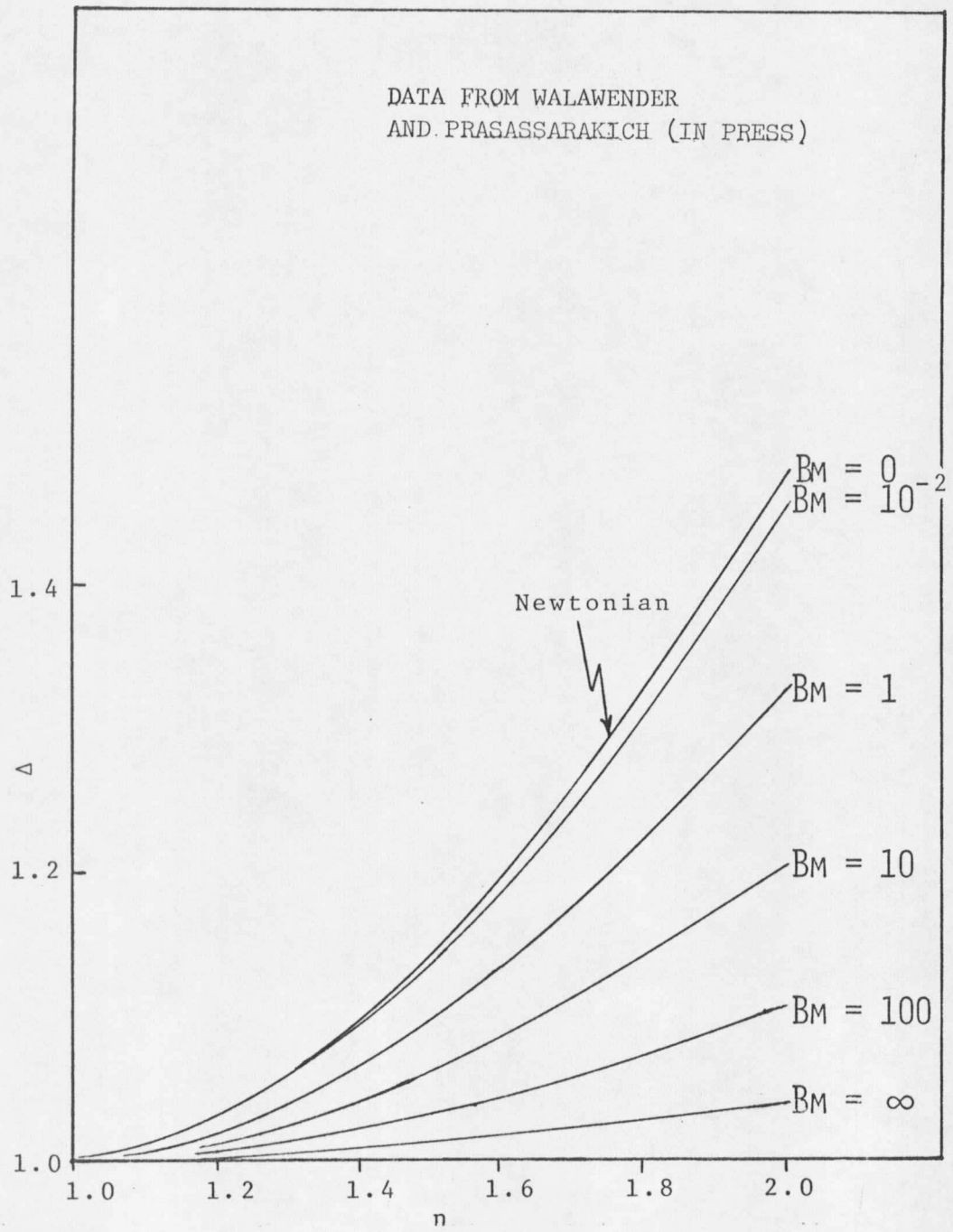


Figure 12. $\frac{\Delta P_{tapered}}{\Delta P_{cylindrical}}$ ($\Delta$) versus $\frac{R_1}{R_2}$ (n)

assumed that the discrepancies between the pressure gradients in the tapered tube and those calculated using the cylindrical approximations can reasonably be neglected. Since this "series of cylinders" model could also be extended to non-Newtonian fluids (contrary to the Newtonian mean diameter model), all further calculations of pressure gradients for branched and tapered tube flow were performed using method two.

Differential Pressures Through the Side Branch
(Water and S-3 Silicone Oil)

Differential measurements were measured through the side branch (B in Figure 3) with the main branch (C in Figure 3) closed off, in an effort to further correlate calculated and experimental values. For this series of runs, both distilled water and S-3 silicone oil were used. Results for both fluids are tabulated in Table XII in which calculated pressures were obtained using the Newtonian mean diameters. Flow rate values for these runs were chosen to correspond to the mean velocity of blood in 160 micron vessels as determined physiologically by Tanaka (1974). For the veins, this value was 1.9 cm/sec, and for the arteries, 2.2 cm/sec. An average of 2.0 cm/sec was used as a typical value and corresponded to a flow rate of .0247 ml/min. Syringe pump flow rates were then chosen as closely as possible to this value

Table XII. Comparison of Measured and Calculated $\Delta P$'s Through Tapered Vessel

L = 1.2 cm D = .0174 cm

| Fluid | V ($cm^3$/min) | $\Delta P_{measured}$ (mm Hg) | $\Delta P_{calculated}$ (mm Hg) | T (C) | $\eta$ (poise) |
|---|---|---|---|---|---|
| S-3 | .118 | 37.51 | 33.79 | 22.7 | .0371 |
| | .0585 | 21.56 | 17.52 | 21.1 | .0388 |
| | .0235 | 7.54 | 6.98 | 21.4 | .0385 |
| $H_2O$ | .118 | 8.24 | 8.87 | 21.2 | .00973 |
| | .118 | 12.97 | 8.96 | 21.8 | .00983 |
| | .0585 | 7.36 | 4.31 | 22.0 | .00955 |
| | .0585 | 5.26 | 4.19 | 23.2 | .00928 |
| | .0235 | 2.46 | 1.75 | 21.5 | .00966 |
| | .0235 | 1.76 | 1.77 | 21.0 | .00978 |

for experimental runs.

Figures 13 and 14 summarize the data in Table XII for S-3 silicone oil and distilled water, respectively. Values for the S-3 silicone oil are all fairly close to the curve; but for water, there was enough variation in experimental data that average values of the measured gradients were used. As can be seen in Table XII, some of the measured pressures for water are very close to the calculated values and others are quite a bit off. This indicates that the experimental apparatus used is probably not sensitive enough to make consistently accurate measurements at the very low pressure gradients associated with water.

Differential Pressures Through the Side Branch (Blood)

Measurements of the pressure gradient through the side branch were next made using suspensions of human RBC's in plasma as the flow medium. As before, the main branch was sealed off so that all of the flow was through the side branch.

The main purpose for this particular set of runs was to show that calculated and measured pressure gradients could be correlated for a non-Newtonian fluid (blood), as was previously done for Newtonian fluids (S-3 silicone oil and distilled water).

Data from this series of runs is tabulated in Table XIII and includes four different feed hematocrits: 24.6%, 30.6%, 36.0%, and

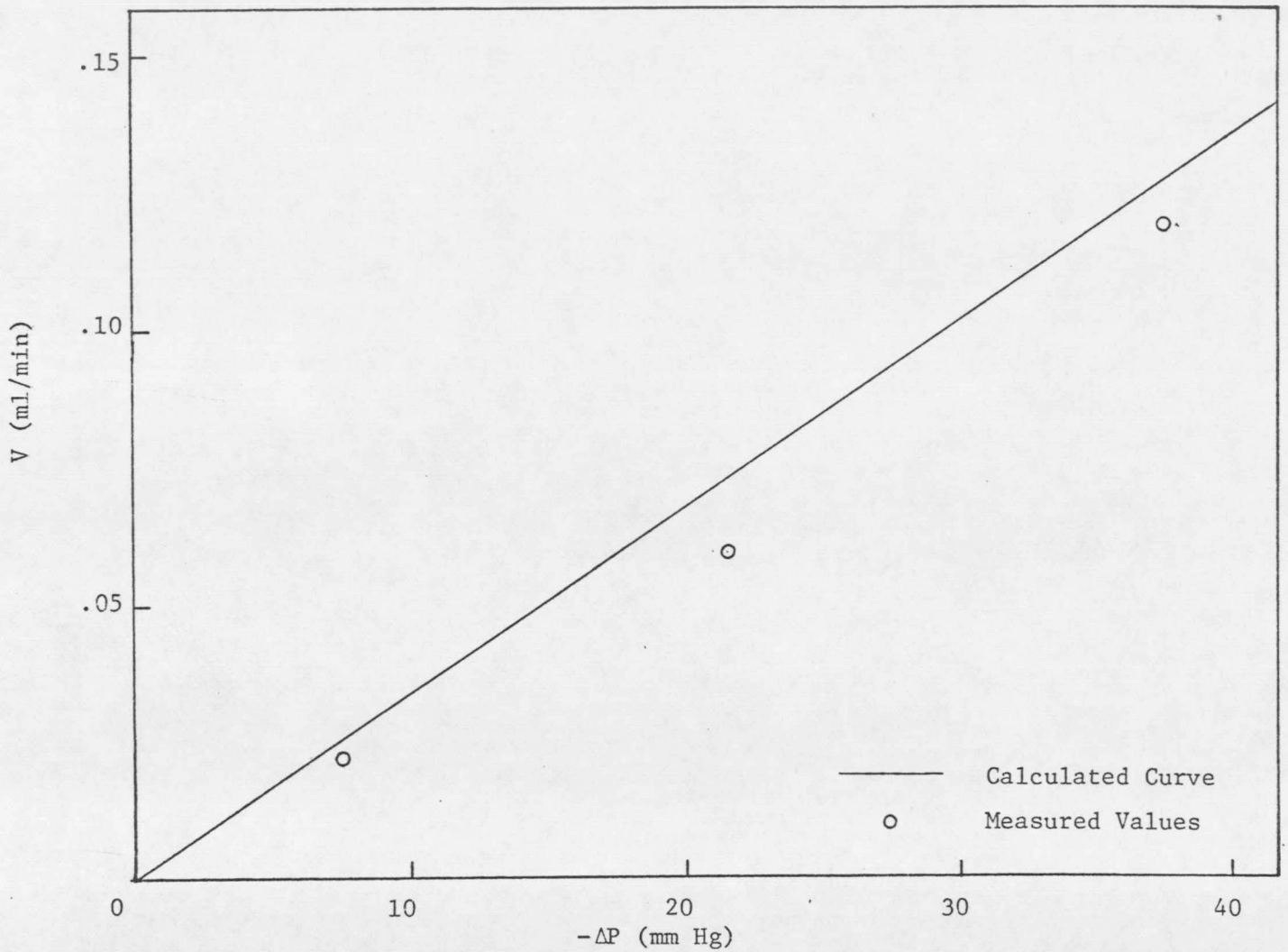


Figure 13. Comparison of $\Delta P_{measured}$ and $\Delta P_{calculated}$ Through a Tapered Vessel (S-3 Silicone Oil)

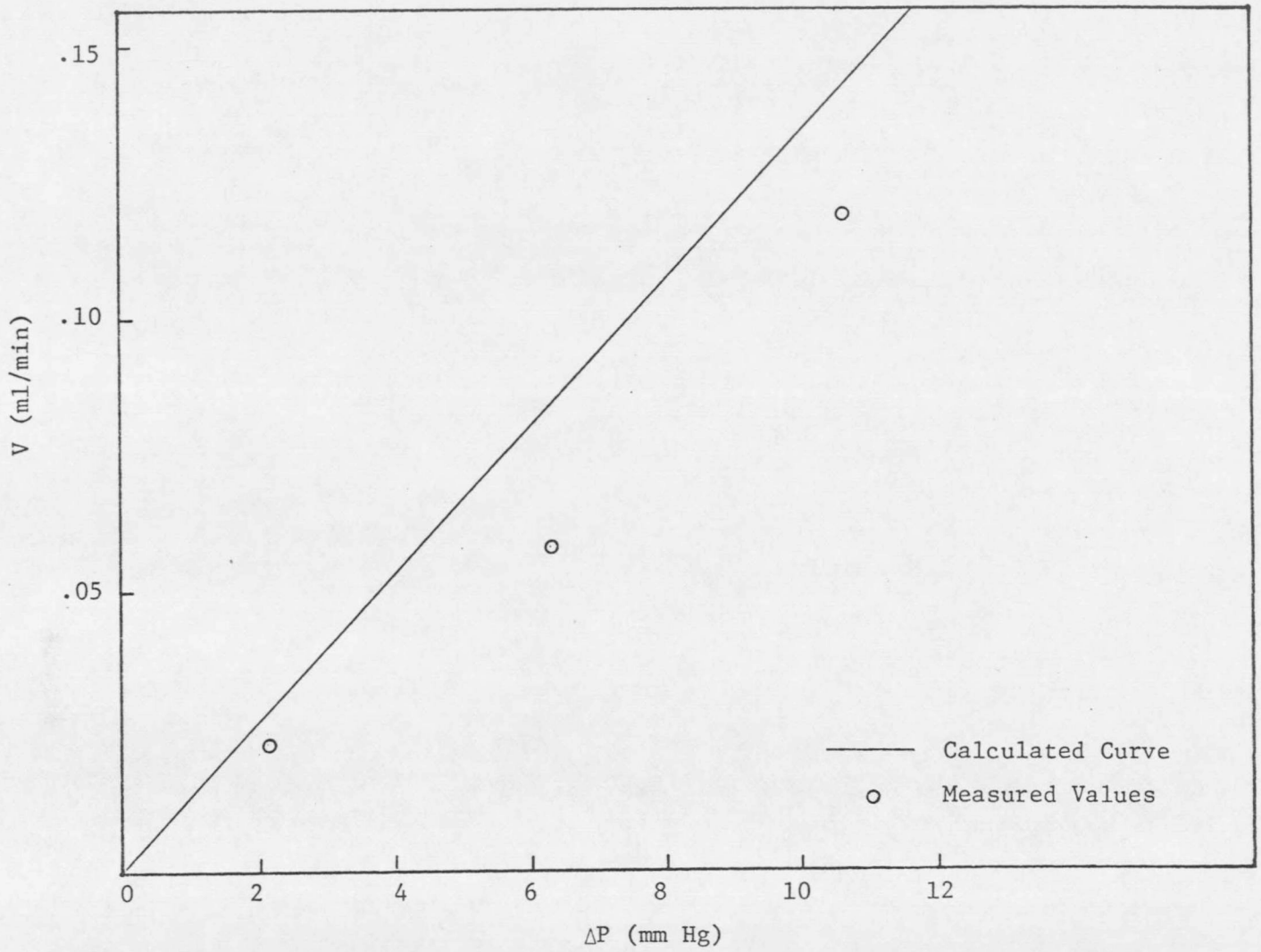


Figure 14. Comparison of $\Delta P_{measured}$ and $\Delta P_{calculated}$ Through a Tapered Vessel (Water)

Table XIII. Comparison of Measured and Calculated ΔP's For Blood Flow Through a Tapered Vessel.

| V ($cm^3$/min) | $\Delta P_{measured}$ (mm Hg) | $\Delta P_{calculated}$ (mm Hg) | $H_{feed}$ (%) | $H_{tube}$ (%) |
|---|---|---|---|---|
| .118 | 20.4 | 24.45 | 24.6 | 22.9 |
| .0585 | 10.3 | 12.05 | 24.6 | 22.9 |
| .0383 | 6.4 | 8.09 | 24.6 | 22.9 |
| .0235 | 3.7 | 5.22 | 24.6 | 22.9 |
| .0154 | 1.8 | 3.59 | 24.6 | 22.9 |
| .118 | 28.9 | 27.43 | 30.5 | 28.4 |
| .0585 | 13.7 | 13.95 | 30.5 | 28.4 |
| .0383 | 8.8 | 9.24 | 30.5 | 28.4 |
| .0235 | 5.7 | 5.93 | 30.5 | 28.4 |
| .0154 | 3.4 | 4.06 | 30.5 | 28.4 |
| .118 | 40.1 | 29.68 | 36.0 | 33.5 |
| .0585 | 19.6 | 15.18 | 36.0 | 33.5 |

Table XIII (Continued).
Comparison of Measured and Calculated ΔP's
For Blood Flow Through a Tapered Vessel.

| V ($cm^3$/min) | $\Delta P_{measured}$ (mm Hg) | $\Delta P_{calculated}$ (mm Hg) | $H_{feed}$ (%) | $H_{tube}$ (%) |
|---|---|---|---|---|
| .118 | 43.1 | 34.06 | 41.5 | 38.6 |
| .0585 | 24.0 | 17.58 | 41.5 | 38.6 |
| .0383 | 12.3 | 11.73 | 41.5 | 38.6 |
| .0383 | 13.7 | 11.73 | 41.5 | 38.6 |
| .0235 | 6.6 | 7.53 | 41.5 | 38.6 |
| .0235 | 11.3 | 7.53 | 41.5 | 38.6 |
| .0154 | 3.7 | 5.24 | 41.5 | 38.6 |
| .0154 | 6.9 | 5.24 | 41.5 | 38.6 |

41.5%. Using the data of Barbee and Cokelet (1971), it can be seen that these feed hematocrits result in tube hematocrits of 22.9%, 28.4%, 33.5%, and 38.6% respectively (see Figure 8) for a tube the size of the side branch (average diameter equal to 174 microns).

Since for this phase of the research the flow rates were in the non-Newtonian region (when using RBC suspensions in plasma), calculated pressures could not be obtained in the same straight-forward manner as before, using Poiseuille's equation. Although shear stress-shear rate data were again obtained using the Wells-Brookfield cone-and-plate viscometer for the higher shear rates, a GDM concentric-cylinder viscometer was also used to obtain similar data in the low shear rate regions. By utilizing the computer programs developed by Bharat Shah for his master's thesis work, the shear stress-shear rate data for a given hematocrit were divided into different ranges and an analytical expression for each range was obtained. Linear regression analysis or non-linear regression analysis was used. From these analytical expressions, integrations were performed to obtain the wall shear stress versus $\overline{U}$ relationship, where $\overline{U}$ is the reduced bulk average velocity. Graphs of these relationships for the four hematocrits being studied are shown in Figures 15, 16, 17, and 18. Each is valid only for the given hematocrit and temperature.

For the tapered side branch, individual $\overline{U}$'s were calculated for each segment of the tube (see Figure 5) by dividing the flow

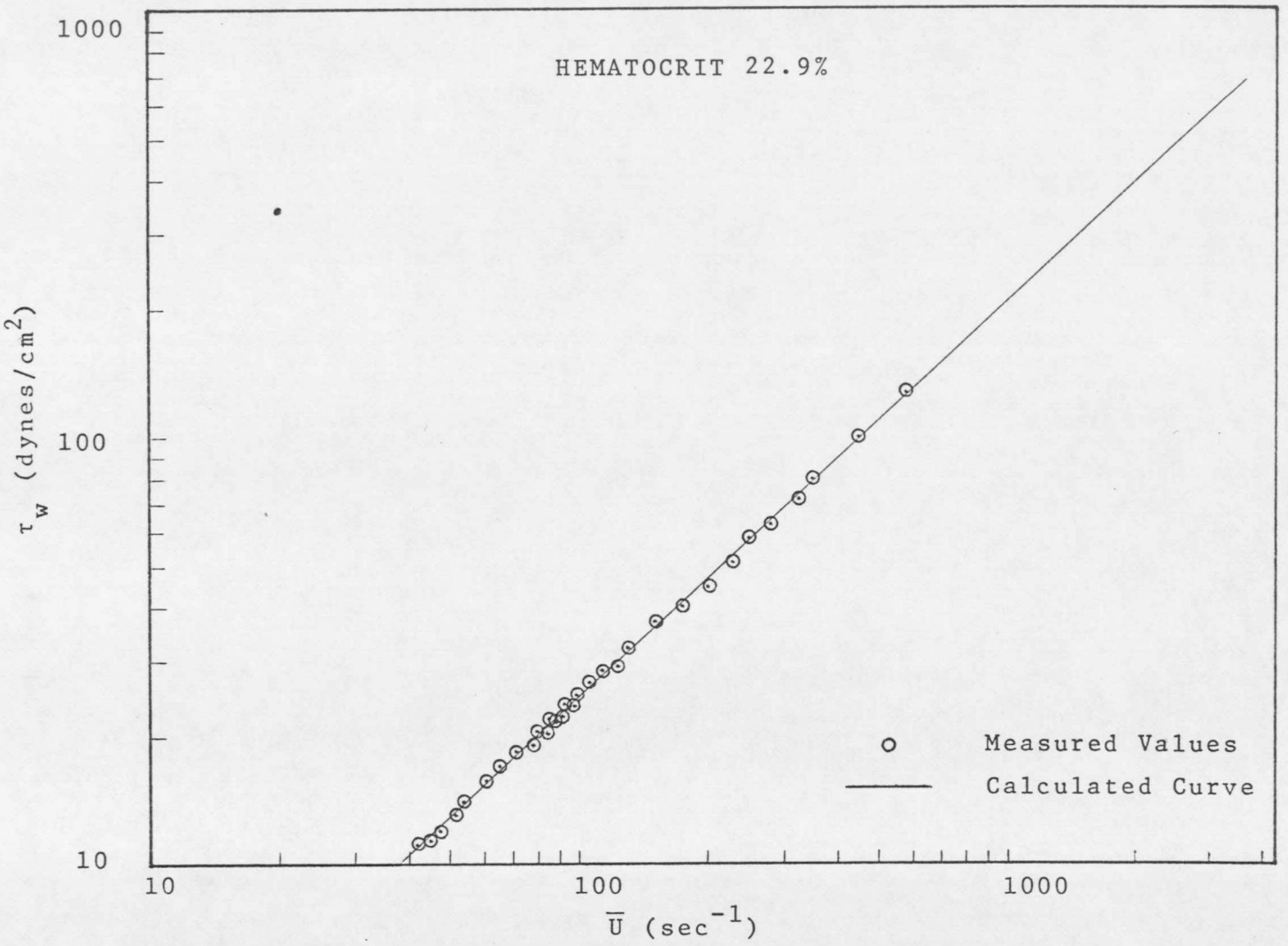


Figure 15. Wall Shear $\tau_w$ versus Reduced Bulk Average Velocity ( $\bar{U}$ )

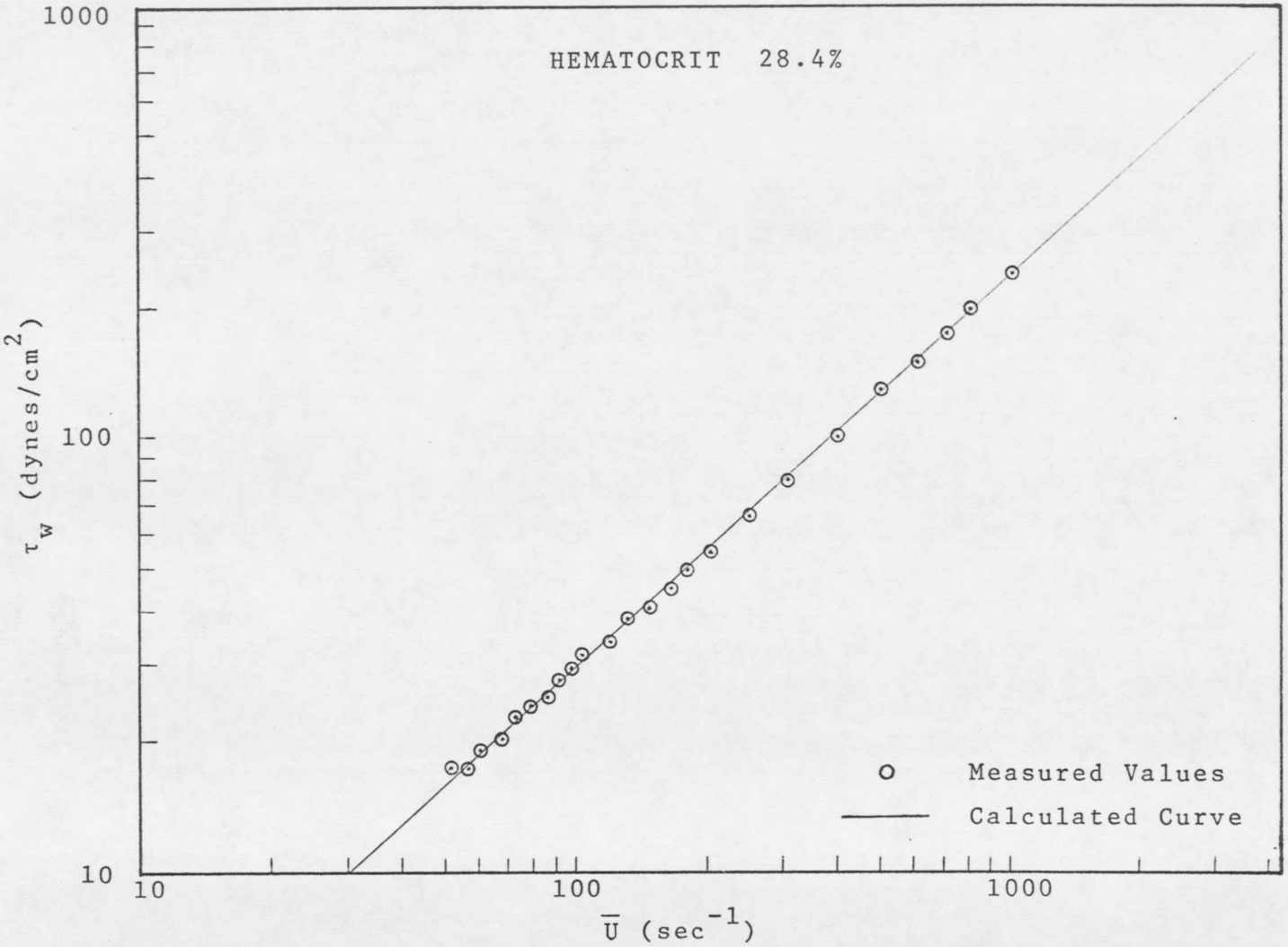


Figure 16. Wall Shear $\tau_w$ versus Reduced Bulk Average Velocity ($\bar{U}$)

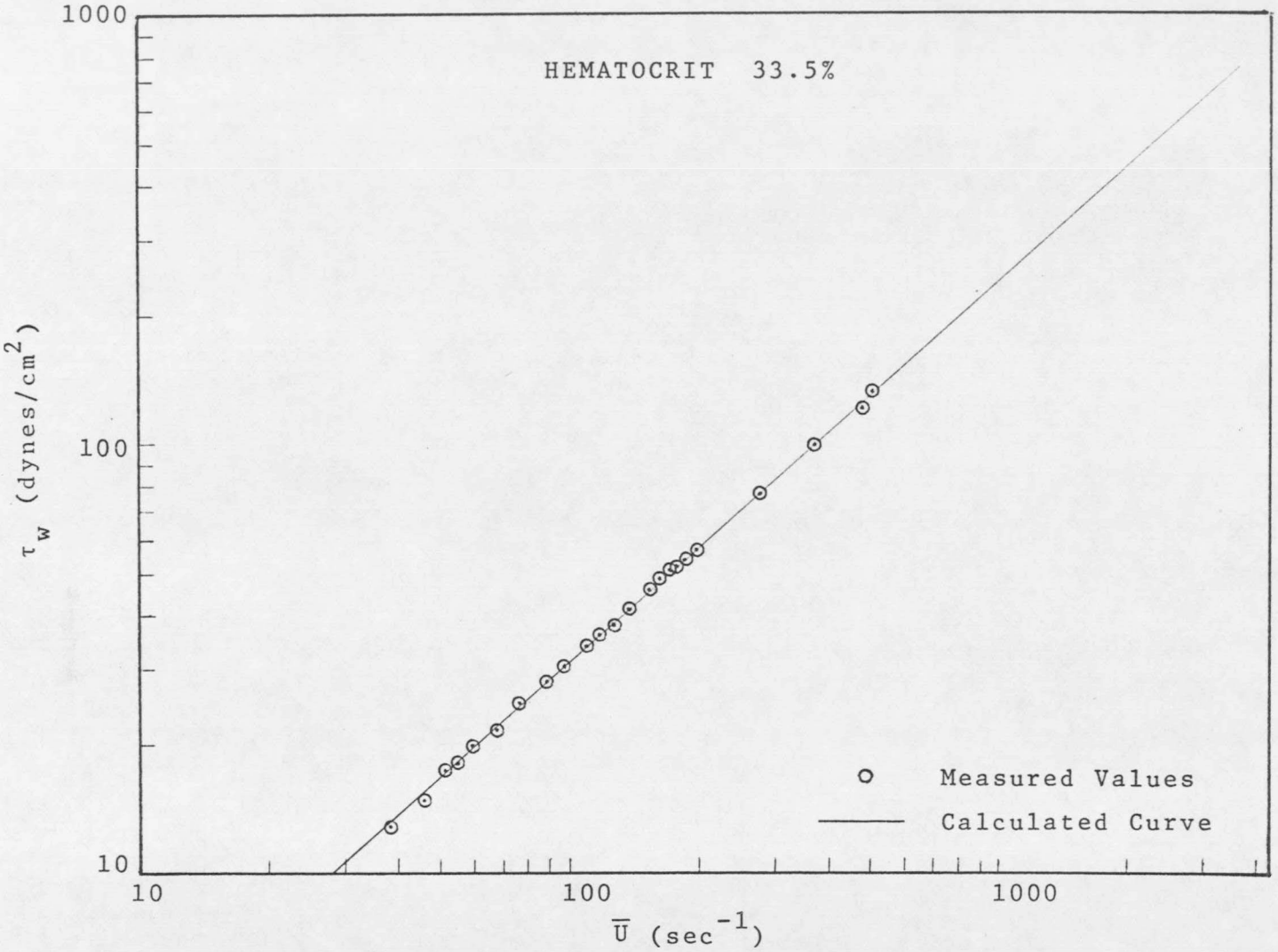


Figure 17. Wall Shear $\tau_w$ versus Reduced Bulk Average Velocity ($\bar{U}$)

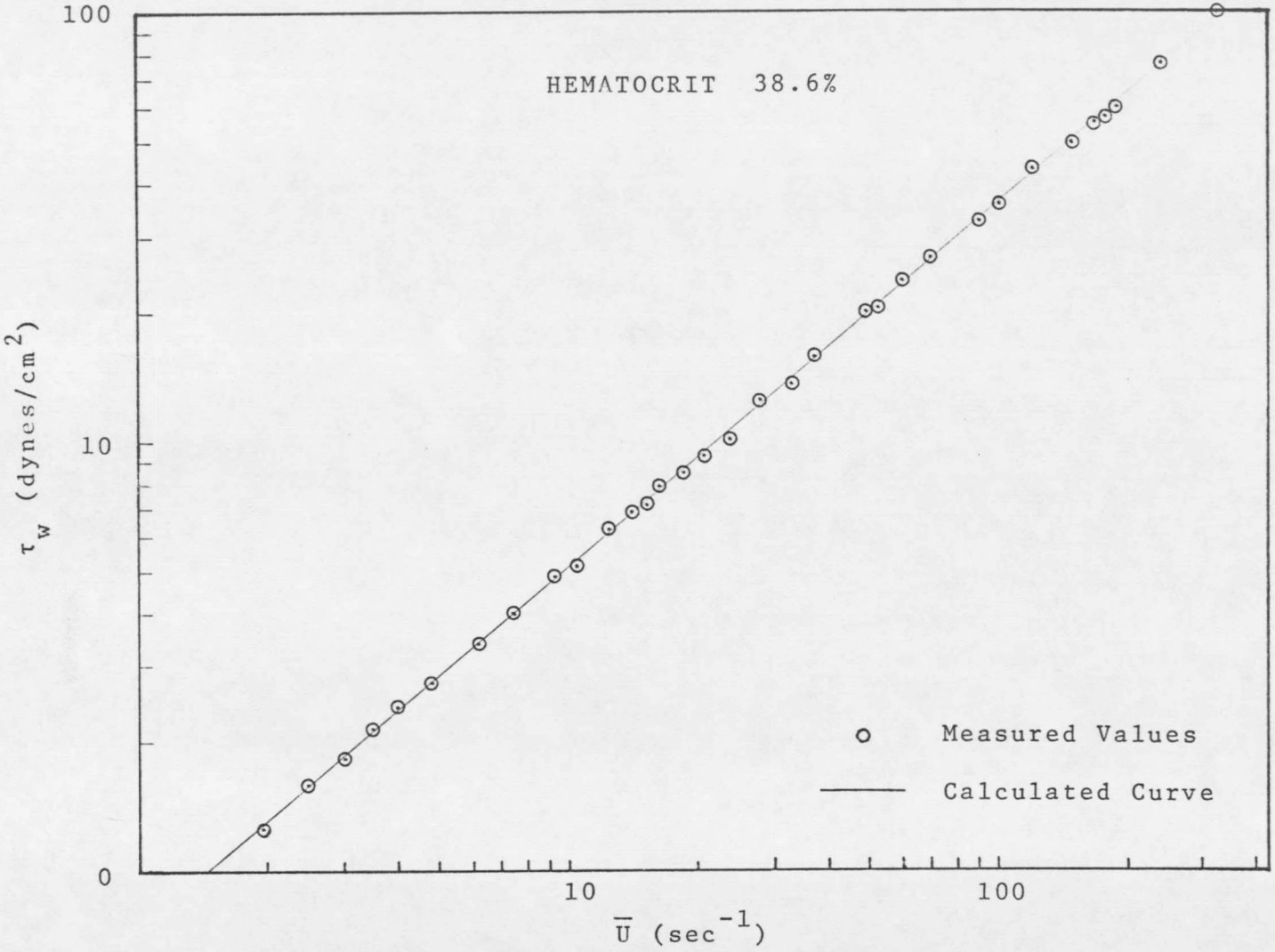


Figure 18. Wall Shear $\tau_w$ versus Reduced Bulk Average Velocity ($\overline{U}$)

rate through the vessel by the average cross-sectional area of each individual segment. Wall shear stress values could then be found using Figures 15 through 18. For steady flow in a rigid, uniform, circular tube, the following relationship applies:

$$\tau_w = \frac{\Delta P \ D}{4 \ L} \qquad (7)$$

so that from known values of the wall shear ($\tau_w$), diameter (D), and length (L); the differential pressure across the segment could be determined. These gradients were then summed to obtain the total pressure drop across the vessel. Values for $\Delta P_{calculated}$, $\Delta P_{measured}$, and flow rate are included in Table XIII as are feed and tube hematocrits.

Figures 19 through 22 presents graphs of pressure gradient versus flow rate for the data of Table XIII. Calculated and measured values are compared for the four tube hematocrits tested. In Figure 19 (hematocrit equal to 22.9%), the measured pressure values all deviate from the calculated line by about the same amount, which could be rationalized by considering the extended period of time required in making GDM viscometer readings for this particular run. This delay would allow the RBC's to crenate, resulting in higher viscosity readings and consequently higher pressure gradients for the calculated curve.

As can be seen in Figure 20 (hematocrit = 28.4%), calculated and measured values coincide as expected. Figures 21 and 22 both show

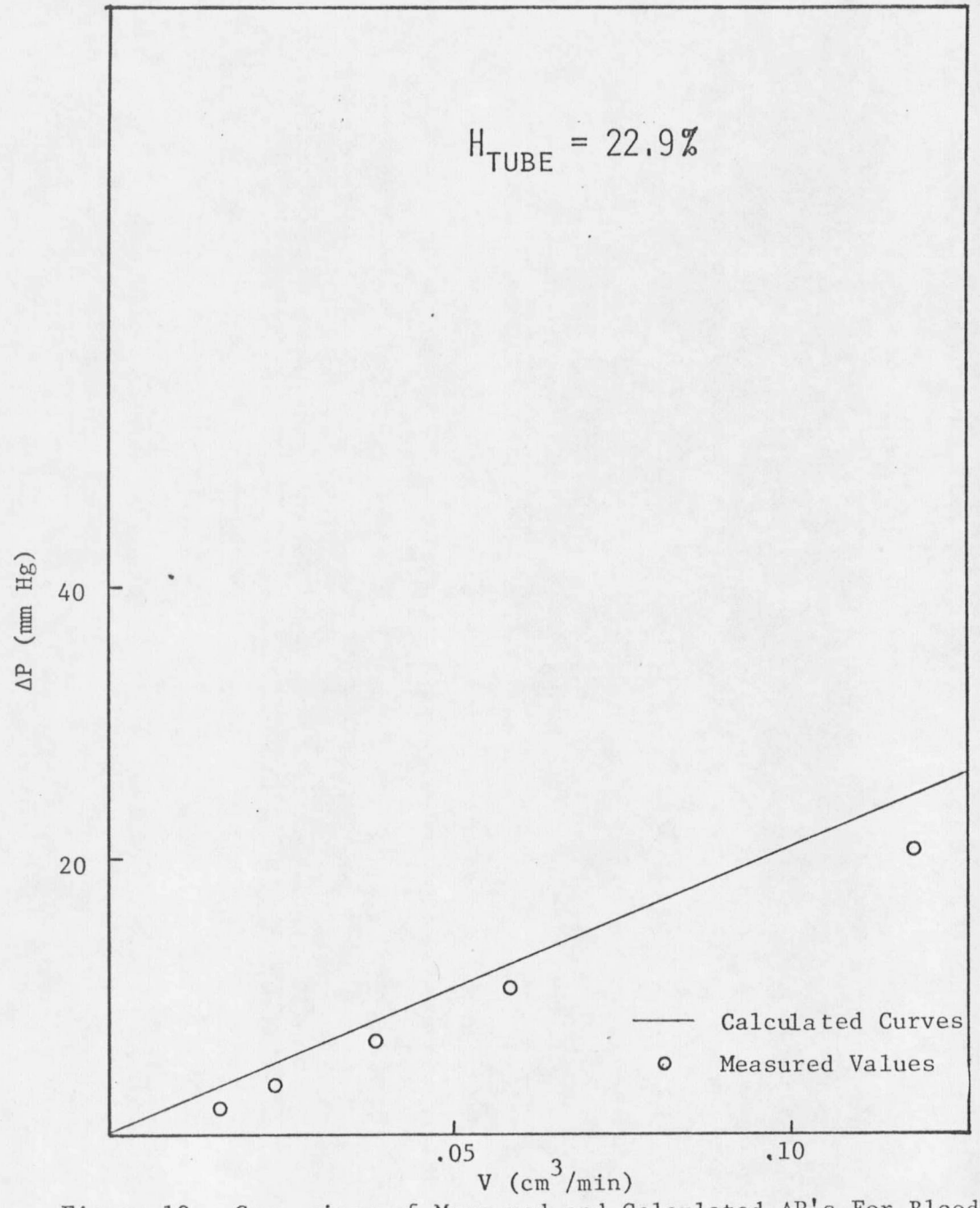


Figure 19. Comparison of Measured and Calculated ΔP's For Blood Flow Through a Tapered Vessel

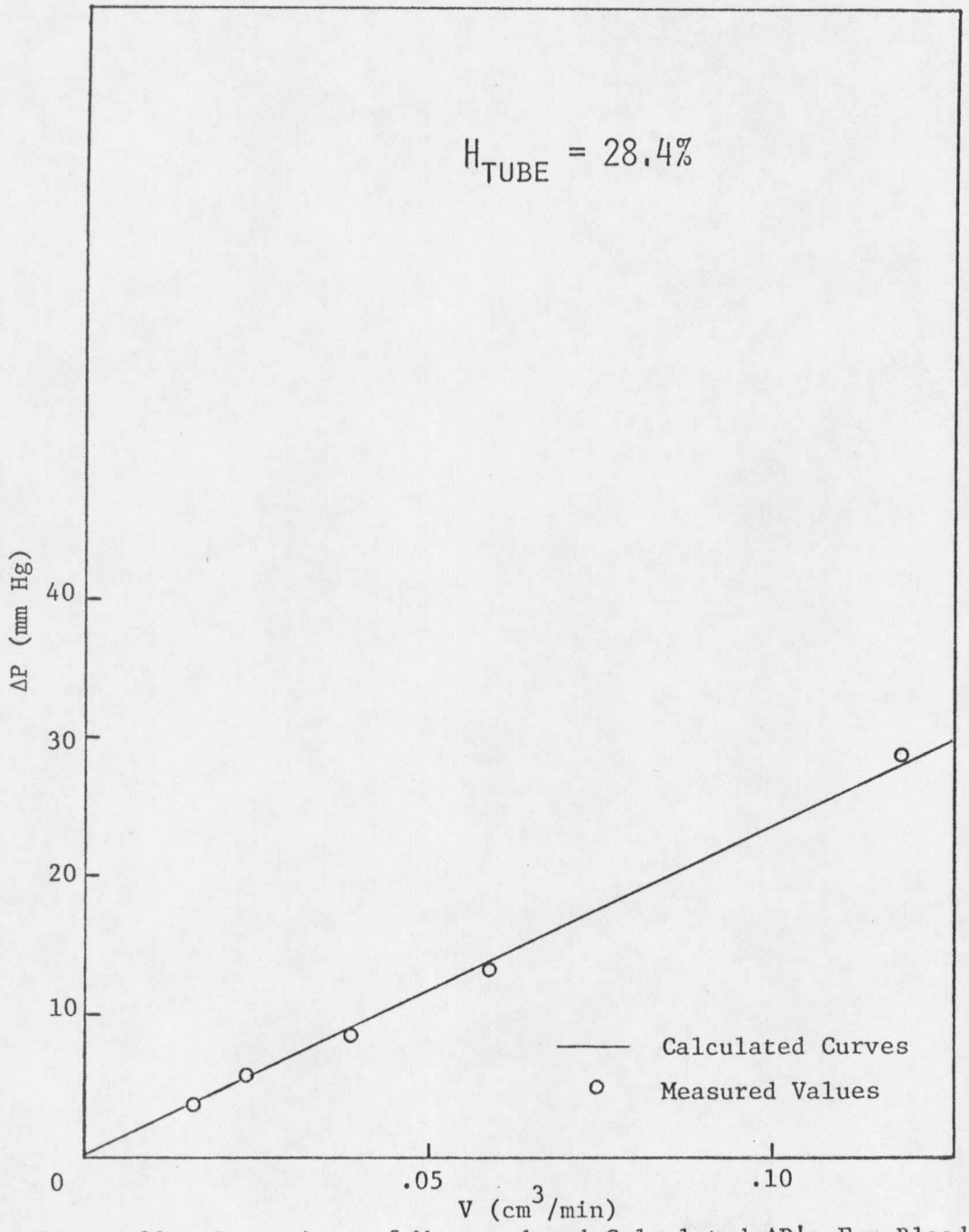


Figure 20. Comparison of Measured and Calculated ΔP's For Blood Flow Through a Tapered Vessel

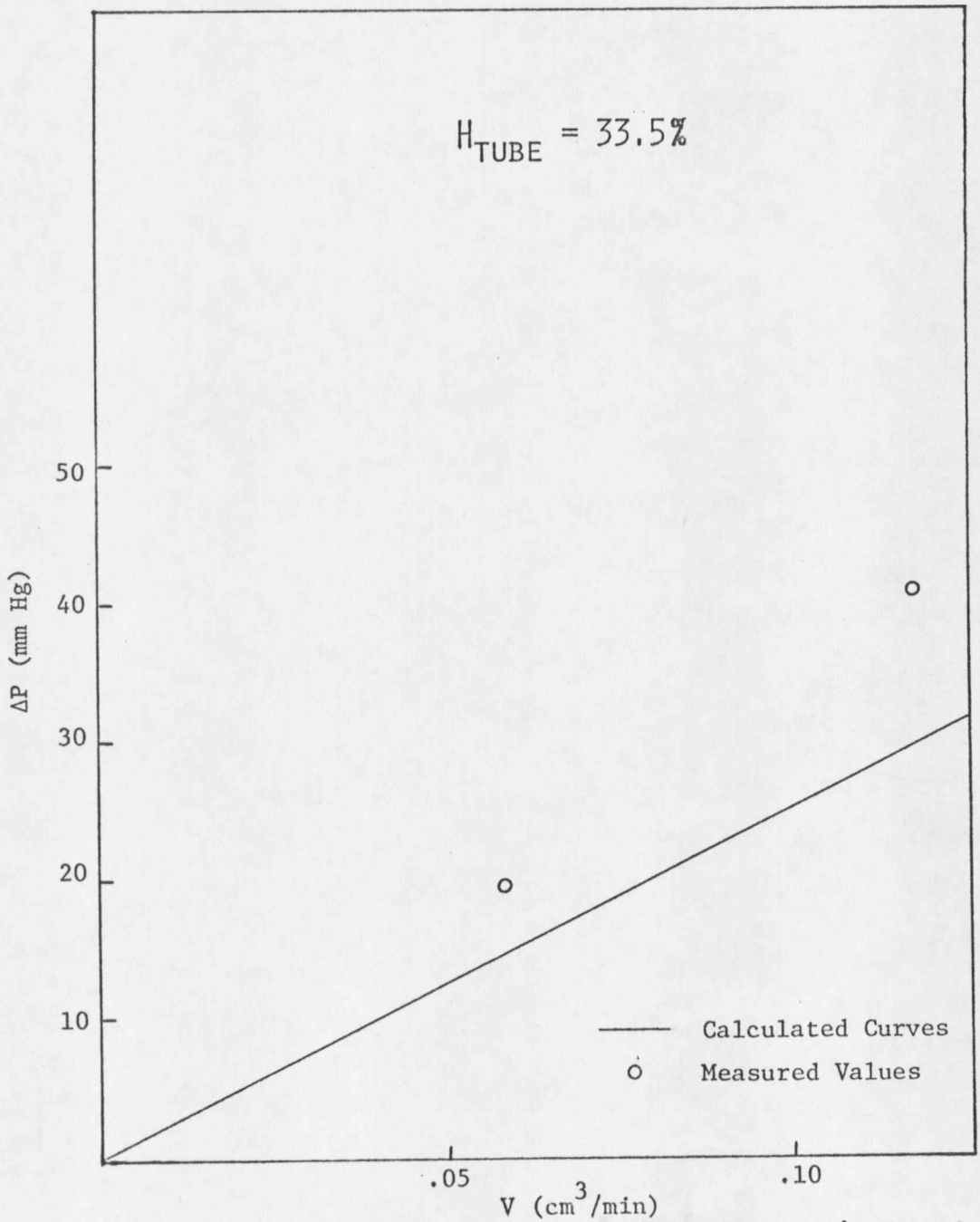


Figure 21. Comparison of Measured and Calculated ΔP's For Blood Flow Through a Tapered Vessel

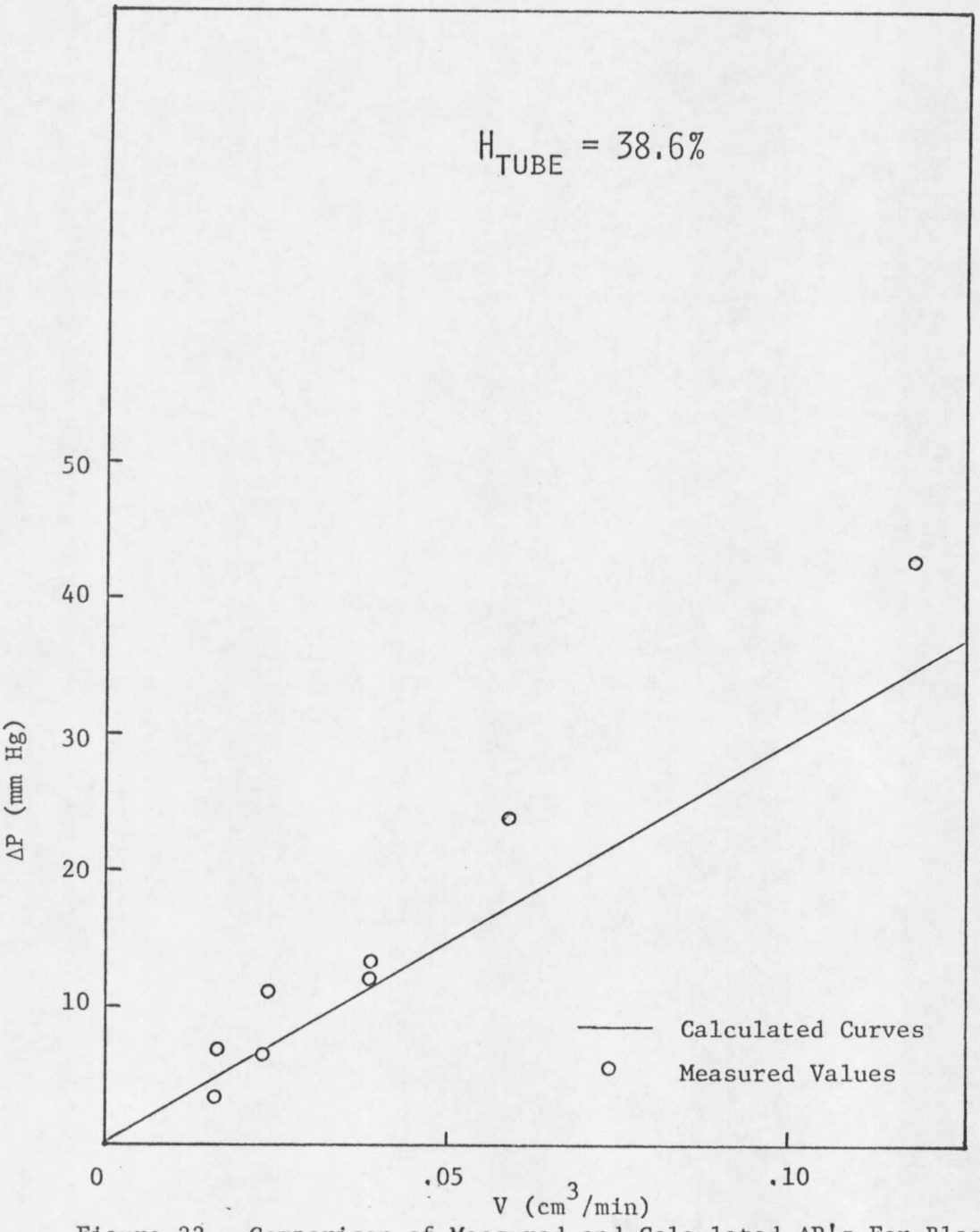


Figure 22. Comparison of Measured and Calculated ΔP's For Blood Flow Through a Tapered Vessel

similar trends of increasingly high measured pressures with respect to calculated pressures, as the flow rate is increased. An explanation for this behavior is not immediately apparent, although it is entirely possible that the experimental technique is at fault. If RBC's were building up at the exit to the vessel, the net effect would be to decrease the vessel diameter, while keeping the flow rate constant. Consequently, measured pressure gradients would be significantly higher than calculated values. As can be seen in Figure 22, some of the measured points fit the curve exactly, while all of the major discrepancies are in the direction predicted by the RBC build-up. In order to eliminate this effect, future work could be performed in an enclosed environment at very high humidity, so that the RBC's would not dry up at the exit of the vessel model.

Pressure Measurements for Branch Flow of Blood

The final phase of this study dealt with the measurement of the pressure drop across the side branch while flow was through both the side and main branches. In addition to plasma, blood cell suspensions with feed hematocrits equal to 30.5% and 41.5% were used as flow media. The major parameter being studied at this point was the ratio of the branch flow to the total flow entering the main and side branches.

Table XIV summarizes the pertinent data for the branched flow run (F is the ratio of branch flow rate to total flow rate) and is shown graphically in Figure 23. As can be seen in this figure, experimental and calculated values are in close agreement for each of the hematocrits used and are almost identical for the plasma runs. (This would be expected for the plasma, since it behaves as a Newtonian fluid.)

A similar study of the phenomena of pressure drop across a bifurcation was presented by Vawter, Fung, and Zweifach (1974), who made a theoretical analysis of the blood flow into a two-dimensional branch. Figure 24 is taken from this study and is a plot of main channel pressure versus distance along the channel (F is the side branch fractional flow). From this figure, it can be seen that the effect of the bifurcation on the channel pressure gradient is a very localized phenomena: i.e., at one branch width from the bifurcation, the pressure gradient is already tending toward constant values.

Vawter also concluded that "the pressure gradient in a channel with a branch is always less than that in a uniform tube without branches." According to in vivo measurements performed by Zweifach (1974), pressure gradients across bifurcations were seen to be in the range of 2-4 mm Hg. Flow rates were so low within the present model's main branch that no appreciable pressure gradient could be measured, so this value could not be directly verified. Vawter, et al., also

Table XIV. Comparison of Measured and Calculated ΔP's For Blood Flowing Across a Bifurcation

| $V_{branch}$ ($cm^3$/min) | F (%) | $H_{feed}$ (%) | $\Delta P_{measured}$ (mm Hg) | $\Delta P_{calculated}$ (mm Hg) |
|---|---|---|---|---|
| .0499 | 20.8 | 41.5 | 16.03 | 15.09 |
| .0856 | 14.2 | 41.5 | 23.65 | 25.26 |
| .0978 | 16.2 | 41.5 | 30.07 | 28.70 |
| .0763 | 12.7 | 41.5 | 39.55 | 22.69 |
| .1159 | 19.3 | 41.5 | 39.55 | 35.46 |
| .0298 | 4.96 | 41.5 | 39.38 | 9.34 |
| .2243 | 36.3 | 41.5 | 58.32 | 61.03 |
| .2028 | 34.0 | 41.5 | 53.25 | 57.31 |
| .1344 | 22.1 | 41.5 | 46.48 | 38.77 |
| .1696 | 28.3 | 41.5 | 50.88 | 48.10 |
| .1847 | 30.5 | 41.5 | 51.89 | 52.07 |
| .1710 | 28.3 | 41.5 | 47.50 | 48.76 |
| .2229 | 36.4 | 30.5 | 45.80 | 50.55 |
| .2001 | 33.8 | 30.5 | 40.56 | 45.57 |
| .1726 | 28.8 | 30.5 | 36.67 | 39.60 |
| .1052 | 17.4 | 30.5 | 30.24 | 24.56 |
| .1153 | 19.1 | 30.5 | 23.65 | 26.92 |

Table XIV. (Continued)
Comparison of Measured and Calculated ΔP's
For Blood Flowing Across a Bifurcation

| $V_{branch}$ ($cm^3$/min) | F (%) | $H_{feed}$ (%) | $\Delta P_{measured}$ (mm Hg) | $\Delta P_{calculated}$ (mm Hg) |
|---|---|---|---|---|
| .0918 | 15.5 | 30.5 | 20.60 | 21.54 |
| .0574 | 9.70 | 30.5 | 17.73 | 13.55 |
| .1179 | 19.7 | 30.5 | 29.57 | 27.41 |
| .1401 | 23.5 | 30.5 | 28.55 | 32.42 |
| .0949 | 15.8 | 30.5 | 19.25 | 22.25 |
| .0814 | 13.7 | 30.5 | 16.20 | 19.17 |
| .0573 | 9.67 | 30.5 | 11.64 | 13.54 |
| .1332 | 22.8 | 0.0 | 16.53 | 16.40 |
| .2391 | 40.8 | 0.0 | 30.47 | 29.43 |
| .1724 | 29.5 | 0.0 | 21.64 | 21.22 |
| .1238 | 21.0 | 0.0 | 15.89 | 15.24 |
| .0818 | 13.9 | 0.0 | 10.66 | 10.07 |

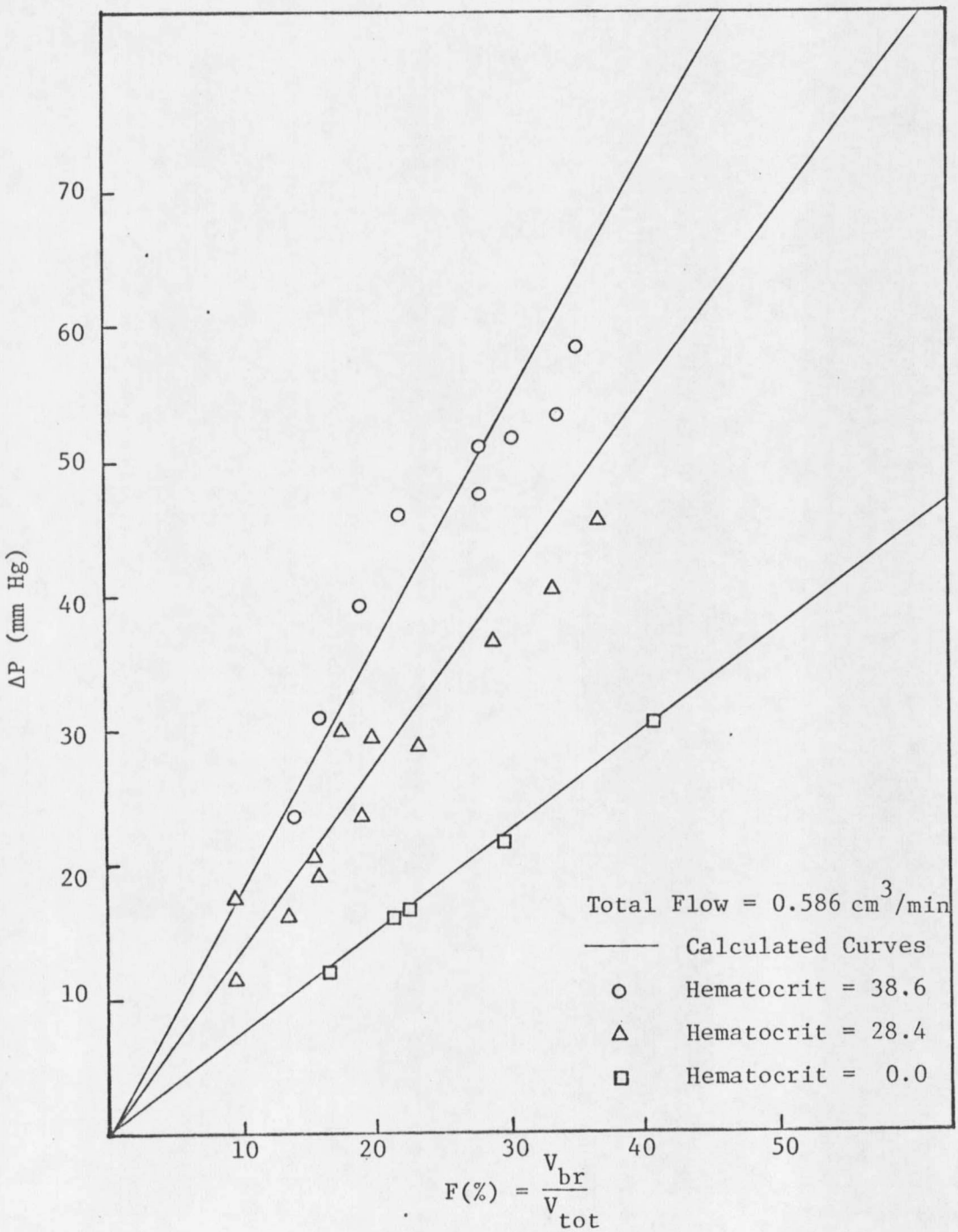


Figure 23. Comparison of Measured and Calculated ΔP's for Blood Flowing Across a Bifurcation

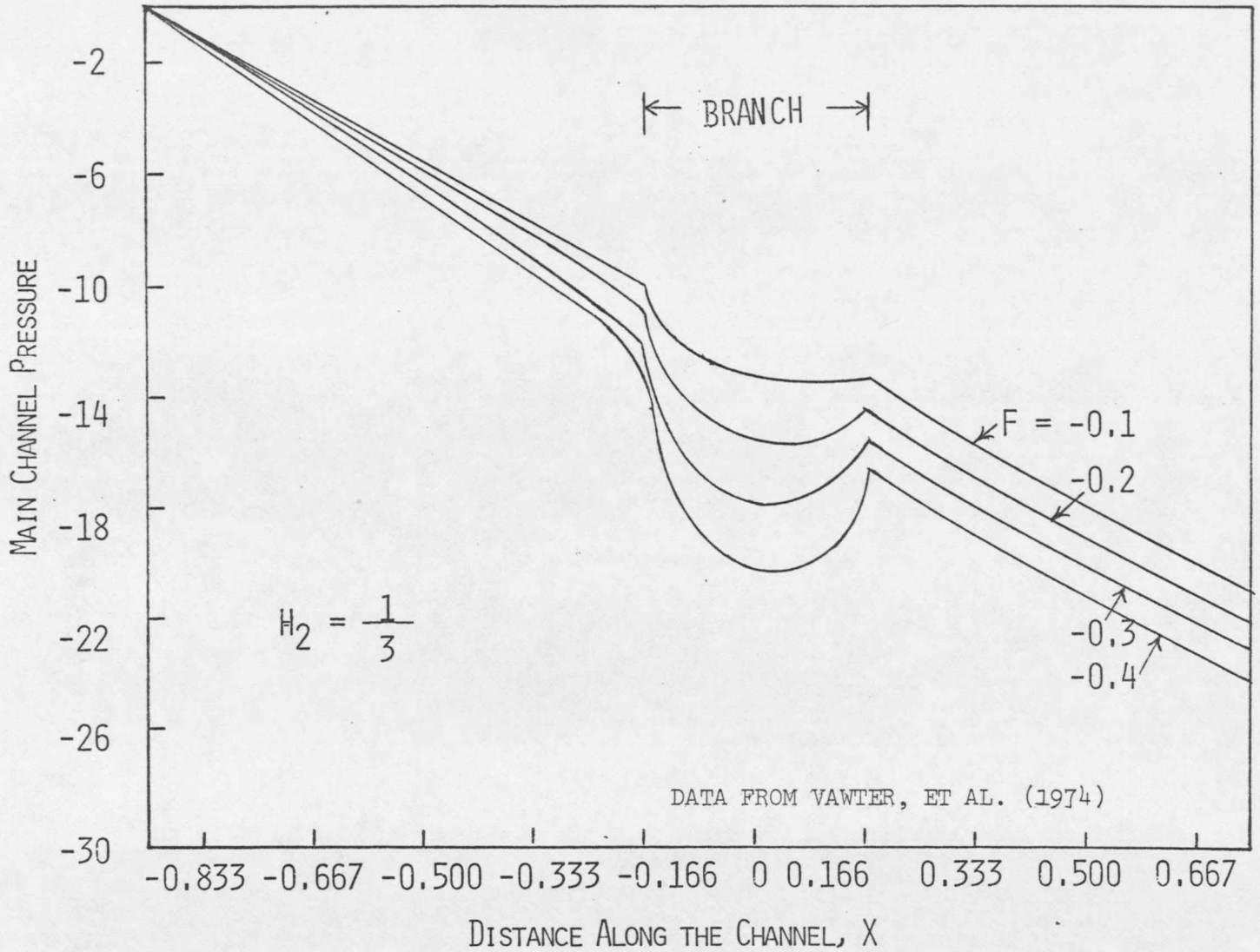


Figure 24. Main Channel Pressure versus Distance Along the Main Channel

predicted (using theoretical grounds), that "the feature of a large pressure drop at the branching point is to be expected over a wide range of flow distribution."

As seen in Figure 23 of the present study, values of the pressure gradient in the side branch (as measured across the bifurcation) are lower than the calculated values in most cases, although this trend cannot be accurately determined from the data because of the presence of so many points on the opposite side of the line. These latter points could be due to the experimental technique, since in several of the experimental runs, it was noted that flow was steadily decreasing in the side branch because of a drying up of the RBC's at the exit of the branch. Runs in which this phenomenon was specifically noted were not used in the analysis of the data, but it is entirely possible that some of the measured pressures included may exhibit this effect. This would result in the discrepancies observed in Figure 23 and could be further investigated by the use of more sophisticated experimental techniques as outlined in the recommendations for further study.

In any case, Vawter's prediction of a large pressure drop at the branching point is not born out by the experimental data available. No interpretation of Figure 23 can possibly support the presence of a large pressure gradient across the bifurcation.

# CONCLUSIONS

Based on the experimental results presented, a number of conclusions may be drawn concerning the use of vascular replicas in the study of pressure flow relationships of human blood:

(1) Plasma skimming is not of significant magnitude to be relevant to pressure flow relationships of blood, in vessel models of the size range studied (diameters equal to ninety microns and above).

(2) Spectrophotometric curves of per cent transmittance versus hematocrit cannot be used to predict the Fahraeus effect in vessels of this size because of the extremely small volumes of blood involved.

(3) The vascular replica could be used to simulate physiological pressure flow relationships which, in turn, could be measured experimentally and calculated mathematically.

(4) Vascular replicas fabricated using an alloy of bismuth, tin, and lead are not suitable for pressure flow studies of this type because of the pitted vessel walls inherent to this metal. If gallium is used however, smooth-walled vessels are obtained.

(5) For steady flow of a Newtonian or non-Newtonian fluid through a non-uniform tapered tube, a "series of cylinders" approach was determined to be a close approximation for calculating pressure gradients across the vessel (for the specific vessel geometries

studied).

(6) Accurate measurements of the vascular replica's diameters could not be obtained using microphotographs taken through the polyester resin surface. Instead, measurements had to be obtained at the completion of the study by physically slicing the model and photographing the lateral sections. This is an extremely inconvenient time to find out the real dimensions of the system in terms of correlating measured and calculated values.

(7) The prediction of a large pressure drop at a bifurcation is not supported by the experimental data, but is instead directly contradicted. Measured values for the gradient across a branch were very close to the values calculated for flow through a straight tube.

# RECOMMENDATIONS FOR FURTHER WORK

Since the initial purpose behind the present study was to investigate the effects of the various parameters influencing plasma skimming, a logical extension of the research would be to obtain vascular replicas in which this effect would be more pronounced, i.e. vessels corresponding to the size range in which plasma skimming has been observed (branch diameters less than about eighty microns). Other models could also be used to further corroborate the results of the present study, in particular those measurements dealing with the pressure gradient across a bifurcation. The necessity for a massive amount of experimental data is indicated in order to fully explore the various parameters involved with network flow in microvascular systems.

According to Vawter, et al. (1974), "the pressure gradient in a channel with a branch is always less than that in a uniform tube without branches". This effect was not measured across the main branch in the present study because of the low pressure gradient but could easily be measured in a later project if larger flow rates or smaller diameter main branches were used to increase this gradient.

As was discussed in the experimental results, a very probable source of error in the experimental technique was the drying up of red blood cells at the exit to the side branch. For future studies,

a means for eliminating this phenomena should be investigated. One possible answer would be to enclose the entire apparatus in a high humidity enviroment, to minimize the effect of evaporation on the exit flow from the side branch. Another would be to have the branch flow empty into a reservoir of saline solution. For this type of setup however, accurate measurements of flow distributions were found to be difficult to obtain, especially at very low flow rates through the side branch.

LITERATURE CITED

1. Barbee, J.H. and G.R. Cokelet. "The Fahraeus Effect." Microvascular Research, Vol. 3, pp. 6-16, 1971.

2. Benis,A. M. and J. Lacoste. "Distribution of Blood Flow in Vascular Beds: Model Study of Geometrical, Rheological and Hydrodynamical Effects." Biorheology, Vol. 5, pp. 147-161, 1968.

3. Bugliarello, G. and G. C. C. Hsiao. "Phase Separation in Suspensions Flowing Through Bifurcations: A Simplified Hemodynamic Model." Science, Vol. 143, pp. 469-471, January, 1964.

4. Cerny,L. C. and W. P. Walawender. "Blood Flow in Rigid Tapered Tubes." Am. J. Physiol. Vol. 210, pp. 341-346, 1966.

5. Charm,S. and G. Kurland. "Blood Flow in Non Uniform Tapered Capillary Tubes." Biorheology, Vol. 4, pp. 175-183, 1967.

6. Cokelet, G. R. and H. J. Meiselman. "Fabrication of Hollow Vascular Replicas using a Gallium Injection Technique." Microvas. Res., Vol. 9, pp. 182-189, 1975.

7. Gelin, L.-E. "A Method for Studies of Aggregation of Blood Cells, Erythrostasis and Plasma Skimming in Branching Capillary Tubes." Biorheology, Vol. 1, pp. 119-127, 1963.

8. Johnson, Paul. "Red Cell Separation in the Mesenteric Capillary Network." Am. J. Physiol., Vol. 221, pp. 99-104, 1971.

9. Kreiger, I. M. and H. Elrod. "Direct Determination of the Flow Curves of Non-Newtonian Fluids--Shearing Rate in the Concentric Cylinder Viscometer." Journal of Applied Physics, Vol. 24, No. 2, pp. 134-136, Feb., 1953.

10. Lawson, H. C. In "Handbook of Physiology" (W. F. Hamilton and P. Dow, Eds.), Sec. 2. Circulation Vol. 1, pp. 23-49; American Physiological Society, Washington,D.C., 1962.

11. Tanaka, Toyoichi. "Blood Velocity Measurement in Human Retinal Vessels." Science, Vol. 186, pp. 830-831, July, 1974.

12. Vawter, D., Y. C. Fung, and B. Zweifach. "Distribution of Blood Flow and Pressure From a Microvessel into a Branch." Microvas. Res., Vol. 8, pp. 44-52, July, 1974.

13. Walawender, W. P. and C. Tien. "Experimental Studies on the Blood Flow Through Tapered Tubes." Int. J. Engng Sci., Vol. 10, pp. 1123-1135, 1972.

14. Walawender, W. P. and P. Prasassarakich. "Flow in Tapering and Cylindrical Vessels." Submitted for publication.

15. Zweifach, B. "Quantitative Studies of Microcirculation Structure and Function." Circ. Res., Vol. 6, pp. 843-857, 1974.

# APPENDIX

## Flow in Tapered Tubes

As presented by Benis and Lacoste (1968), it can be assumed that the wall shear stress is a function only of $\overline{U}$, L, and D for steady flow in a uniform, rigid, circular tube. Also, $\tau_w = \Delta PD/4L$ for steady flow in a tube. Thus, we have:

$$\tau_w = \frac{D}{4}(dP/dL) = f(\overline{U},D,L) \qquad (A1)$$

where D is a function of L. The total pressure drop across any non-uniform tube is then obtained by integration of equation (A1), such that

$$\Delta P = 4 \int_{L_1}^{L_2} [f(\overline{U},D,L)/D]\, dL \qquad (A2)$$

If it is assumed that (a) $\tau_w$ is a function of $\overline{U}$ only, and (b) the taper is uniform so that $dL = [L/(D_2-D_1)]\, dD$, then equation (A2) becomes:

$$\Delta P = \frac{4L}{D_2-D_1} \int_{D_1}^{D_2} [f(\overline{U})/D]\, dD. \qquad (A3)$$

Since $\overline{U} = 4V/\pi D^3$, equation (A3) can be integrated for the Newtonian case (where $\tau_w = 8\eta\overline{U}$) to obtain:

$$\frac{\Delta P}{L} = \frac{128\eta V}{\pi D_{NM}^4} \tag{A4}$$

where:

$$D_{NM}^4 = \frac{3(D_2-D_1)}{D_1^{-3}-D_2^{-3}} \tag{A5}$$

Equations (A4) and (A5) can now be used for the calculation of the total pressure drop across any non-uniform tube.

Terminology for this derivation is as follows:

$\eta$ = Newtonian viscosity

L = tube length

D = tube diameter

$\Delta P$ = pressure gradient across the tube

V = volumetric flow rate

$\tau_w$ = wall shear stress

$\overline{U}$ = reduced bulk average velocity

Fenton, Bruce M
Flow of human blood through fabricated replicas of microvascular bifurcations

| DATE | ISSUED TO |
| --- | --- |
| | |
| | |
| | |
| | |
| | |
| | |
| | |
| | |
| | |
| | |
| | |